methylation," which has also been seen with other genes (e.g., APC). In any case, the observed correlation between FKBP6 methylation and breast cancer stage suggests that methylation of FKBP6 could be a molecular marker for advanced breast cancer.

In summary, we have screened targets of DNA methylation in breast cancers and identified nine genes silenced by methylation. NTN4, PGP9.5, and DKK3 genes are methylated in cancer-specific manner and could be useful molecular markers for diagnosing breast cancer. Introduction of NTN4 cDNA into breast cancer cells suppressed tumor growth, suggesting NTN4 could be a novel tumor suppressor in breast cancer. More broadly, identification of genes silenced by DNA methylation in breast cancer may provide valuable information that not only contributes to our understanding of the pathogenesis of the disease, but also to the development of new strategies for diagnosis and therapy.

Acknowledgments The authors thank Dr. William F. Goldman for editing the manuscript. This study was supported in part by Grants-in-Aid for Scientific Research on Priority Areas from the Ministry of Education, Culture, Sports, Science, and Technology (K.I., T.T., and M.T.), Grants-in-Aid for Scientific Research (S) from Japan Society for Promotion of Science (K.I.), a Grant-in-Aid for the Third-term Comprehensive 10-year Strategy for Cancer Control, and Grant-in-Aid for Cancer Research from the Ministry of Health, Labor, and Welfare, Japan (M.T.).

References

1. Bird A (1992) The essentials of DNA methylation. Cell 70:5–8
2. Jones PA, Baylin SB (2007) The epigenomics of cancer. Cell 128:683–692
3. Jemal A, Siegel R, Ward E et al (2008) Cancer statistics, 2008. CA Cancer J Clin 58:71–96
4. Schuebel KE, Chen W, Cope L et al (2007) Comparing the DNA hypermethylome with gene mutations in human colorectal cancer. PLoS Genet 3:1709–1723
5. Herman JG, Merlo A, Mao L et al (1995) Inactivation of the CDKN2/p16/MTS1 gene is frequently associated with aberrant DNA methylation in all common human cancers. Cancer Res 55:4525–4530
6. Ferguson AT, Evron E, Umbricht CB et al (2000) High frequency of hypermethylation at the 14-3-3 sigma locus leads to gene silencing in breast cancer. Proc Natl Acad Sci USA 97:6049–6054
7. Graff JR, Herman JG, Lapidus RG et al (1995) E-cadherin expression is silenced by DNA hypermethylation in human breast and prostate carcinomas. Cancer Res 55:5195–5199
8. Krop IE, Sgroi D, Porter DA et al (2001) HIN-1, a putative cytokine highly expressed in normal but not cancerous mammary epithelial cells. Proc Natl Acad Sci USA 98:9796–9801
9. Dammann R, Yang G, Pfeifer GP (2001) Hypermethylation of the cpG island of Ras association domain family 1A (RASSF1A), a putative tumor suppressor gene from the 3p21.3 locus, occurs in a large percentage of human breast cancers. Cancer Res 61:3105–3109
10. Conway KE, McConnell BB, Bowring CE et al (2000) TMS1, a novel proapoptotic caspase recruitment domain protein, is a target of methylation-induced gene silencing in human breast cancers. Cancer Res 60:6236–6242
11. Rodriguez BA, Cheng AS, Yan PS et al (2008) Epigenetic repression of the estrogen-regulated Homeobox B13 gene in breast cancer. Carcinogenesis 29:1459–1465
12. Douglas DB, Akiyama Y, Carraway H et al (2004) Hypermethylation of a small CpGuanine-rich region correlates with loss of activator protein-2alpha expression during progression of breast cancer. Cancer Res 64:1611–1620
13. Chung W, Kwabi-Addo B, Ittmann M et al (2008) Identification of novel tumor markers in prostate, colon and breast cancer by unbiased methylation profiling. PLoS One 3:e2079
14. Ostrow KL, Park HL, Hoque MO et al (2009) Pharmacologic unmasking of epigenetically silenced genes in breast cancer. Clin Cancer Res 15:1184–1191
15. Tommasi S, Karm DL, Wu X et al (2009) Methylation of homeobox genes is a frequent and early epigenetic event in breast cancer. Breast Cancer Res 11:R14
16. Gardiner-Garden M, Frommer M (1987) CpG islands in vertebrate genomes. J Mol Biol 196:261–282
17. Clark SJ, Harrison J, Paul CL et al (1994) High sensitivity mapping of methylated cytosines. Nucleic Acids Res 22:2990–2997
18. Watanabe Y, Toyota M, Kondo Y et al (2007) PRDM5 identified as a target of epigenetic silencing in colorectal and gastric cancer. Clin Cancer Res 13:4786–4794
19. Yang AS, Estecio MR, Doshi K et al (2004) A simple method for estimating global DNA methylation using bisulfite PCR of repetitive DNA elements. Nucleic Acids Res 32:e38
20. Sasaki Y, Morimoto I, Ishida S et al (2001) Adenovirus-mediated transfer of the p53 family genes, p73 and p51/p63 induces cell cycle arrest and apoptosis in colorectal cancer cell lines: potential application to gene therapy of colorectal cancer. Gene Ther 8:1401–1408
21. Sasaki Y, Negishi H, Koyama R et al (2009) p53 family members regulate the expression of the apolipoprotein D gene. J Biol Chem 284:872–883
22. Suzuki H, Igarashi S, Nojima M et al (2009) IGFBP7 is a p53 responsive gene specifically silenced in colorectal cancer with CpG island methylator phenotype. Carcinogenesis. doi:10.1093/carcin/bgp179
23. Kim MS, Lebron C, Nagpal JK et al (2008) Methylation of the DFNA5 increases risk of lymph node metastasis in human breast cancer. Biochem Biophys Res Commun 370:38–43
24. Veeck J, Bektas N, Hartmann A et al (2008) Wnt signalling in human breast cancer: expression of the putative Wnt inhibitor Dickkopf-3 (DKK3) is frequently suppressed by promoter hypermethylation in mammary tumours. Breast Cancer Res 10:R82
25. Veeck J, Niederacher D, An H et al (2006) Aberrant methylation of the Wnt antagonist SFRP1 in breast cancer is associated with unfavourable prognosis. Oncogene 25:3479–3488
26. Akino K, Toyota M, Suzuki H et al (2007) Identification of DFNA5 as a target of epigenetic inactivation in gastric cancer. Cancer Sci 98:88–95
27. Mandelker DL, Yamashita K, Tokumaru Y et al (2005) PGP9.5 promoter methylation is an independent prognostic factor for esophageal squamous cell carcinoma. Cancer Res 65:4963–4968
28. Sato H, Suzuki H, Toyota M et al (2007) Frequent epigenetic inactivation of DICKKOPF family genes in human gastrointestinal tumors. Carcinogenesis 28:2459–2466
29. Suzuki H, Watkins DN, Jair KW et al (2004) Epigenetic inactivation of SFRP genes allows constitutive WNT signaling in colorectal cancer. Nat Genet 36:417–422

30. Wu G, Guo Z, Chang X et al (2007) LOXL1 and LOXL4 are epigenetically silenced and can inhibit ras/extracellular signal-regulated kinase signaling pathway in human bladder cancer. Cancer Res 67:4123–4129
31. Lejmi E, Leconte L, Pedron-Mazoyer S et al (2008) Netrin-4 inhibits angiogenesis via binding to neogenin and recruitment of Unc5B. Proc Natl Acad Sci USA 105:12491–12496
32. Micale L, Fusco C, Augello B et al (2008) Williams-Beuren syndrome TRIM50 encodes an E3 ubiquitin ligase. Eur J Hum Genet 16:1038–1049
33. Crackower MA, Kolas NK, Noguchi J et al (2003) Essential role of Fkbp6 in male fertility and homologous chromosome pairing in meiosis. Science 300:1291–1295
34. Marchesani M, Hakkarainen A, Tuomainen TP et al (2003) New paraoxonase 1 polymorphism I102V and the risk of prostate cancer in Finnish men. J Natl Cancer Inst 95:812–818
35. Lehto M, Mayranpaa MI, Pellinen T et al (2008) The R-Ras interaction partner ORP3 regulates cell adhesion. J Cell Sci 121:695–705
36. Masuda Y, Futamura M, Kamino H et al (2006) The potential role of DFNA5, a hearing impairment gene, in p53-mediated cellular response to DNA damage. J Hum Genet 51:652–664
37. Arakawa H (2004) Netrin-1 and its receptors in tumorigenesis. Nat Rev Cancer 4:978–987
38. Suzuki H, Toyota M, Carraway H et al (2008) Frequent epigenetic inactivation of Wnt antagonist genes in breast cancer. Br J Cancer 98:1147–1156
39. Tokumaru Y, Yamashita K, Kim MS et al (2008) The role of PGP9.5 as a tumor suppressor gene in human cancer. Int J Cancer 123:753–759
40. Yamashita K, Park HL, Kim MS et al (2006) PGP9.5 methylation in diffuse-type gastric cancer. Cancer Res 66:3921–3927
41. Karpf AR, Peterson PW, Rawlins JT et al (1999) Inhibition of DNA methyltransferase stimulates the expression of signal transducer and activator of transcription 1, 2, and 3 genes in colon tumor cells. Proc Natl Acad Sci USA 96:14007–14012
42. Issa JP, Ahuja N, Toyota M et al (2001) Accelerated age-related CpG island methylation in ulcerative colitis. Cancer Res 61: 3573–3577
43. Kwabi-Addo B, Chung W, Shen L et al (2007) Age-related DNA methylation changes in normal human prostate tissues. Clin Cancer Res 13:3796–3802
44. Shen L, Toyota M, Kondo Y et al (2007) Integrated genetic and epigenetic analysis identifies three different subclasses of colon cancer. Proc Natl Acad Sci USA 104:18654–18659
45. Nojima M, Suzuki H, Toyota M et al (2007) Frequent epigenetic inactivation of SFRP genes and constitutive activation of Wnt signaling in gastric cancer. Oncogene 26:4699–4713
46. Rattner A, Hsieh JC, Smallwood PM et al (1997) A family of secreted proteins contains homology to the cysteine-rich ligand-binding domain of frizzled receptors. Proc Natl Acad Sci USA 94:2859–2863
47. Bafico A, Liu G, Goldin L et al (2004) An autocrine mechanism for constitutive Wnt pathway activation in human cancer cells. Cancer Cell 6:497–506
48. Schlosshauer PW, Brown SA, Eisinger K et al (2000) APC truncation and increased beta-catenin levels in a human breast cancer cell line. Carcinogenesis 21:1453–1456
49. Van Laer L, Huizing EH, Verstreken M et al (1998) Nonsyndromic hearing impairment is associated with a mutation in DFNA5. Nat Genet 20:194–197
50. Thompson DA, Weigel RJ (1998) Characterization of a gene that is inversely correlated with estrogen receptor expression (ICERE-1) in breast carcinomas. Eur J Biochem 252:169–177
51. Lage H, Helmbach H, Grottke C et al (2001) DFNA5 (ICERE-1) contributes to acquired etoposide resistance in melanoma cells. FEBS Lett 494:54–59
52. Esseghir S, Kennedy A, Seedhar P et al (2007) Identification of NTN4, TRA1, and STC2 as prognostic markers in breast cancer in a screen for signal sequence encoding proteins. Clin Cancer Res 13:3164–3173
53. Toyota M, Suzuki H, Yamashita T et al (2009) Cancer epigenomics: implications of DNA methylation in personalized cancer therapy. Cancer Sci 100:787–791
54. Meng X, Lu X, Morris CA et al (1998) A novel human gene FKBP6 is deleted in Williams syndrome. Genomics 52:130–137

Published OnlineFirst October 26, 2010; DOI:10.1158/1078-0432.CCR-10-0581

Human Cancer Biology

Clinical Cancer Research

A Novel Correlation between *LINE-1* Hypomethylation and the Malignancy of Gastrointestinal Stromal Tumors

Shinichi Igarashi[1], Hiromu Suzuki[1,2], Takeshi Niinuma[1], Haruo Shimizu[1,8], Masanori Nojima[1,3], Hiroyuki Iwaki[9], Takayuki Nobuoka[4], Toshirou Nishida[10,11], Yasuaki Miyazaki[11], Hiroyuki Takamaru[1], Eiichiro Yamamoto[1,2], Hiroyuki Yamamoto[1], Takashi Tokino[5], Tadashi Hasegawa[6], Koichi Hirata[4], Kohzoh Imai[7], Minoru Toyota[2], and Yasuhisa Shinomura[1]

Abstract

Purpose: Gastrointestinal stromal tumors (GIST) are the most important mesenchymal tumors of the gastrointestinal tract. The vast majority of GISTs exhibit activating mutations of *KIT* or *PDGFRA*, but epigenetic alteration of GISTs is largely unknown. In this study, we aimed to clarify the involvement of DNA methylation in GIST malignancy.

Experimental Design: A total of 106 GIST specimens were studied. Levels of *LINE-1* methylation were analyzed using bisulfite pyrosequencing. In addition, methylation of three other repetitive sequences (*Alu Yb8*, Satellite-α, and *NBL2*) was similarly analyzed, and CpG island hypermethylation was analyzed using MethyLight. Array-based comparative genomic hybridization (array CGH) was carried out in 25 GIST specimens.

Results: *LINE-1* hypomethylation was significantly correlated with risk, and high-risk GISTs exhibited significantly lower levels of *LINE-1* methylation than low-risk (61.3% versus 53.2%; $P = 0.001$) or intermediate-risk GISTs (60.8% versus 53.2%; $P = 0.002$). Hypomethylation of Satellite-α and *NBL2* was also observed in high-risk GISTs. By contrast, promoter hypermethylation was relatively infrequent (*CDH1*, 11.2%; *MLH1*, 9.8%; *SFRP1*, 1.2%; *SFRP2*, 11.0%; *CHFR*, 9.8%; *APC*, 6.1%; *CDKN2A*, 0%; *RASSF1A*, 0%; *RASSF2*, 0%) and did not correlate with *LINE-1* methylation or risk. Array CGH analysis revealed a significant correlation between *LINE-1* hypomethylation and chromosomal aberrations.

Conclusions: Our data suggest that *LINE-1* hypomethylation correlates significantly with the aggressiveness of GISTs and that *LINE-1* methylation could be a useful marker for risk assessment. Hypomethylation may increase the malignant potential of GISTs by inducing accumulation of chromosomal aberrations. *Clin Cancer Res; 16(21); 5114–23. ©2010 AACR.*

Gastrointestinal stromal tumors (GIST), which consist of a spectrum of both benign and malignant tumors, constitute the most important group of primary mesenchymal tumors of the gastrointestinal tract (1, 2). Immunohistochemically, GISTs are positive for KIT and CD34 and are negative or variably positive for other neural and smooth muscle cell markers. The expression of KIT and CD34 is a characteristic feature of the intestinal cells of Cajal (ICC), which are located in the intestinal wall and regulate gastrointestinal motility. GISTs are thus thought to originate from ICCs or ICC precursors. Activating *KIT* mutations have been identified in 80% to 90% of GISTs, and mutation of the platelet-derived growth factor receptor α gene (*PDGFRA*) is observed in ~5% of GISTs (1–3). In that context, imatinib (formerly STI571) was developed as a tyrosine kinase inhibitor and has been shown to inhibit BCR-ABL, KIT, and PDGFR activities (1–3). Imatinib is currently being used for the treatment of both chronic myeloid leukemia and metastatic GISTs.

Authors' Affiliations: [1]First Department of Internal Medicine, Sapporo Medical University; [2]Department of Biochemistry, Sapporo Medical University; [3]Department of Public Health, Sapporo Medical University; [4]First Department of Surgery, Sapporo Medical University; [5]Department of Molecular Biology, Cancer Research Institute, Sapporo Medical University; [6]Department of Surgical Pathology, Sapporo Medical University; [7]The Advanced Clinical Research Center, The Institute of Medical Science, The University of Tokyo, Tokyo, Japan; [8]Department of Gastroenterology, Muroran General Hospital, Muroran, Japan; [9]Department of Pathology, Sunagawa City Medical Center, Sunagawa Japan; and [10]Department of Surgery, Osaka Police Hospital; [11]Department of Surgery, Osaka University Graduate School of Medicine, Osaka, Japan

Note: Supplementary data for this article are available at Clinical Cancer Research Online (http://clincancerres.aacrjournals.org/).

S. Igarashi and H. Suzuki contributed equally to this work.

Corresponding Authors: Shinomura Yasuhisa, First Department of Internal Medicine, Sapporo Medical University, S1, W16, Chuo-ku, Sapporo 060-8543, Japan. Phone: 81-11-611-2111; Fax: 81-11-611-2282; E-mail: shinomura@sapmed.ac.jp. or Minoru Toyota, Department of Biochemistry, Sapporo Medical University, S1, W17, Chuo-ku, Sapporo 060-8556, Japan. Phone: 81-11-611-2111; Fax: 81-11-622-1918; E-mail: mtoyota@sapmed.ac.jp.

doi: 10.1158/1078-0432.CCR-10-0581

Published OnlineFirst October 26, 2010; DOI:10.1158/1078-0432.CCR-10-0581

Translational Relevance

Gastrointestinal stromal tumors (GIST) are the most important mesenchymal tumors of the gastrointestinal tract. Predicting the biological potential of GISTs is often difficult, and discovery of molecular markers to predict the malignant potential of GISTs is essential. In this study, we provide compelling evidence for the association between *LINE-1* hypomethylation and the aggressiveness of GISTs. Using quantitative bisulfite pyrosequencing analysis, we found that high-risk GISTs exhibit significantly lower *LINE-1* methylation levels than low- or intermediate-risk GISTs. We further show a novel correlation between *LINE-1* hypomethylation and increases in chromosomal losses and gains. To our knowledge, this is the first study to show that *LINE-1* methylation could be a useful marker for the risk assessment of GISTs, and that hypomethylation may increase the malignant potential of GISTs by inducing chromosomal instability.

Predicting the biological potential of GISTs is often difficult, and considerable effort has been made to define the variables that would enable more accurate identification of tumors with malignant potential. In most classification systems, key prognostic factors for estimating malignant potential are tumor size and mitotic rate, and, to a more variable degree, the proliferation index or tumor site (1, 2, 4). Other potential and promising markers of GIST malignancy are molecular alterations. As mentioned, the vast majority of GISTs exhibit activating *KIT* or *PDGFRA* mutations. By itself, however, the mutation status does not fully explain the diverse biology of GISTs, and it is believed that additional molecular alterations are required for the progression of high-risk GISTs.

Neoplasias are thought to arise through the accumulation of multiple genetic and epigenetic alterations. Two contradicting epigenetic events coexist in cancer: global hypomethylation, which is mainly observed in repetitive sequences within the genome, and regional hypermethylation, which is frequently associated with CpG islands within gene promoters (5). Hypermethylation of CpG islands is a common feature of cancer that is associated with gene silencing (5, 6). In contrast to CpG islands, repetitive DNA elements are normally heavily methylated in somatic tissues. About 45% of the human genome is composed of repetitive sequences, including long interspersed nuclear element (LINE) and short interspersed nuclear element (SINE; ref. 7), and an earlier study has shown that methylation of such repetitive elements can serve as a surrogate for global methylcytosine content (8). Moreover, *LINE-1* hypomethylation is known to occur during the development of various human malignancies (9–13), and we recently reported that *LINE-1* methylation is diminished in enlarged fold gastritis, which is a risk factor of gastric cancer (14). Hypomethylation of Alu elements and other repetitive sequences also has been observed in tumors of various origin (15–20). To date, however, only a few groups have reported epigenetic abnormalities in GISTs (21–24), and there are no published studies of *LINE-1* methylation in GISTs.

Our aim in the present study was to assess the contribution made by epigenetic alterations to the malignant potential of GISTs. We quantitatively analyzed levels of *LINE-1* methylation, and also assessed CpG island hypermethylation in a panel of tumor-associated genes in primary GIST specimens. In addition, we carried out an array-based comparative genomic hybridization (array CGH) analysis to examine the relation between chromosomal aberrations and *LINE-1* hypomethylation in GISTs.

Materials and Methods

Patients and tumor tissues

A total of 106 GIST specimens were obtained from Sapporo Medical University Hospital, Sunagawa City Medical Center, Muroran General Hospital, and Osaka University Hospital. Informed consent was obtained from all patients before collection of the specimens, and this study was approved by the respective institutional review boards. Risk grade was assessed according to the risk definition system proposed by Fletcher et al. (4). Tumors that were <2 cm in diameter with a mitotic count of <5/50 high-power fields (HPF) were categorized as very low risk. Tumors that were 2 to 5 cm in diameter with <5 mitotic count/50 HPF were considered to be low risk. Tumors that were <5 cm in diameter with a mitotic count of 6 to 10/50 HPF, or were 5 to 10 cm with a mitotic count <5/50 HPF, were considered to be intermediate risk. Tumors that were >5 cm in diameter with a mitotic count of >5/50 HPF, >10 cm in diameter with any mitotic count, or any size with a mitotic count of >10/50 HPF were considered to be high risk. Genomic DNA was extracted from formalin-fixed, paraffin-embedded tissue specimens using a QIAamp DNA FFPE Tissue kit (Qiagen). Genomic DNA was extracted from fresh-frozen tissue specimens using the standard phenol-chloroform procedure.

Bisulfite pyrosequencing

Genomic DNA (1 μg) was modified with sodium bisulfite using an EpiTect Bisulfite kit (Qiagen), and bisulfite pyrosequencing analysis was done as described previously (14). Briefly, PCR was run in a 25-μL volume containing 50 ng of bisulfite-treated DNA, 1× MSP buffer [67 mmol/L Tris-HCl (pH 8.8), 16.6 mmol/L $(NH_4)_2SO_4$, 6.7 mmol/L $MgCl_2$, and 10 mmol/L 2-mercaptoethanol], 1.25 mmol/L deoxynucleotide triphosphate, 0.4 μmol/L each primer, and 0.5 unit of JumpStart REDTaq DNA Polymerase (Sigma-Aldrich). The PCR protocol for bisulfite sequencing entailed 5 minutes at 95°C; 40 cycles of 1 minute at 95°C, 1 minute at 60°C, and 1 minute at 72°C; and a 7-minute final extension at 72°C. The biotinylated PCR product was purified, made single stranded, and used as a template in a pyrosequencing reaction run according to the manufacturer's

Published OnlineFirst October 26, 2010; DOI:10.1158/1078-0432.CCR-10-0581

instructions. The PCR products were bound to Streptavidin Sepharose HP beads (Amersham Biosciences), after which beads containing the immobilized PCR product were purified, washed, and denatured using a 0.2 mol/L NaOH solution. After addition of 0.3 μmol/L sequencing primer to the purified PCR product, pyrosequencing was carried out using a PSQ96MA system (Biotage) and Pyro Q-CpG software (Biotage). Primer sequences for *LINE-1* methylation were as described (14). Primer sequences for *Alu Yb8*, centromeric satellite-α of chromosome 1 (*Sat-α*), and *NBL2* were as described (20).

MethyLight assay

Genomic DNA (1 μg) was modified with sodium bisulfite as described above. PCR was run in a 20-μL volume containing 50 ng of bisulfite-treated DNA, 625 nmol/L each primer, 250 nmol/L Taqman-MGB probe, and 1× Taqman Fast Universal PCR Master Mix (Applied Biosystems). Fast real-time PCR was done using a 7500 Fast Real-Time PCR System according to the manufacturer's instructions (Applied Biosystems). The PCR protocol entailed 20 seconds at 95°C followed by 40 cycles of 3 seconds at 95°C and 30 seconds at 60°C. We used Alu as a normalization control reaction (25). Primers, probes, and the percentage of methylated reference (PMR) were as described previously (26, 27). We used a PMR cutoff of 4 to distinguish methylation-positive (PMR > 4) from methylation-negative (PMR ≤ 4) samples (27).

Array-based comparative genomic hybridization

Microarray-based CGH analysis was done according to the manufacturer's instructions (Agilent Technologies). Briefly, 500 ng of genomic DNA from fresh-frozen GIST specimens and gender-matched reference DNA (Promega) were digested with *Alu*I and *Rsa*I before labeling and hybridization. Using a Genomic DNA Enzymatic Labeling kit (Agilent Technologies), tumor DNA and reference DNA were labeled with Cy5 and Cy3, respectively. Before hybridization, labeled DNA was mixed with 25 μg of Cot-1 DNA (Invitrogen), denatured at 95°C for 3 minutes, and incubated at 37°C for 30 minutes to block repetitive sequences. The probe mixture was then hybridized for 40 hours at 65°C to a Human Genome CGH Microarray Kit 105A (G4412A; Agilent Technologies), which contains ~99,000 probes annotated against National Center for Biotechnology Information Build 36. After washing, the array was scanned with an Agilent G2565BA Microarray Scanner, and the fluorescent signals were acquired using Feature Extraction software (Agilent Technologies). The ADM-2 algorithm included in the DNA Analytics 4.0 software (Agilent Technologies) was used to identify DNA copy number aberrations. A copy number loss was defined as a $\log_2$ ratio <−0.5, and a copy number gain was defined as a $\log_2$ ratio >0.5. All genomic positions were defined according to the University of California Santa Cruz Human version hg18. The Gene Expression Omnibus accession numbers of the microarray data are GSM552402, GSM552403, GSM552404, GSM552405, GSM552406, GSM552407, GSM552408, GSM552409, GSM552410, GSM552411, GSM552412, GSM552413, GSM552414, GSM552415, GSM552416, GSM552417, GSM552418, GSM552419, GSM552420, GSM552421, GSM552422, GSM552423, GSM552424, GSM552425, and GSM552426, and the accession number of the Series entry is GSE22185.

Statistical analysis

Mean methylation levels were compared using *t* tests or one-way ANOVA with a post hoc Games-Howell test. Methylation levels were correlated with other biological features by calculating the Pearson's and Spearman's correlation coefficients. *LINE-1* methylation levels were categorized into four groups: greater than 1 SD (1 − SD) above the mean, plus/minus 1 − SD from the mean, and less than 1 − SD below the mean. Sex- and age-adjusted odds ratios (OR) for high-risk category were then calculated using logistic regression models. *P* values of <0.05 (two-sided) were considered significant. Statistical analyses were carried out using Statistical Package for the Social Sciences software 15.0J (SPSS, Inc.) and StatView (SAS Institute, Inc.).

Results

Clinicopathologic characteristics

The clinicopathologic features of the 106 patients with primary GISTs are summarized in Table 1. The majority of the GISTs were located in the stomach (65%) and small intestine (27%), and the mean tumor size was 6.9 cm (range, 0.5-22 cm). The risk classification proposed by Fletcher et al. (4) was available for 85 patients. Of those,

Table 1. Clinicopathologic features of the GIST samples used in this study

Age (y, median ± SD)	68.0 ± 14.1
Gender	
Male	53 (50.0%)
Female	53 (50.0%)
Tumor location	
Stomach	68 (64.8%)
Small intestine	28 (26.7%)
Omentum	4 (3.8%)
Colon	3 (2.8%)
Esophagus	2 (1.9%)
Tumor size (cm, average ± SD)	6.92 ± 41.0
Mitotic count (/50 HPF, average ± SD)	7.1 ± 11.7
Risk category (*n* = 85)	
Very low	1 (1.2%)
Low	23 (27.1%)
Intermediate	19 (22.3%)
High	42 (49.4%)
Metastasis in high-risk group (*n* = 42)	
Absent	28 (66.7%)
Present	14 (33.3%)

Published OnlineFirst October 26, 2010; DOI:10.1158/1078-0432.CCR-10-0581

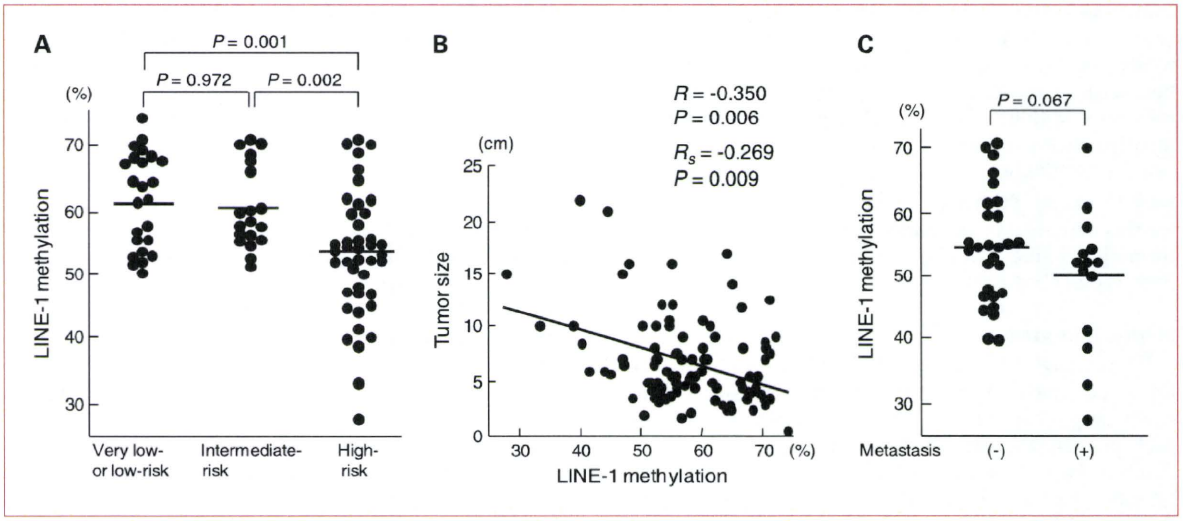

Fig. 1. Analysis of *LINE-1* methylation in GISTs. A, comparison of the levels of *LINE-1* methylation among low-risk (n = 23), intermediate-risk (n = 19), and high-risk (n = 42) GISTs. Filled circles depict the average methylation (%) at multiple CpG sites. B, correlation of *LINE-1* methylation with tumor size. The Pearson's correlation coefficient (R) and the Spearman correlation coefficient (Rs) are shown. C, comparison of *LINE-1* methylation between high-risk GISTs with and without metastasis.

1 (1.2%) was classified as very low risk, 23 (27.1%) were low risk, 19 (22.3%) were intermediate risk, and 42 (49.4%) were high risk. Among the 42 patients in the high-risk group, metastasis was found in 14 (33.3%).

Hypomethylation of *LINE-1* in GISTs

We next asked whether global DNA hypomethylation is involved in the development of GISTs. To address this question, we carried out bisulfite pyrosequencing to quantitatively analyze *LINE-1* promoter methylation as a surrogate for global methylcytosine content. All of the samples were analyzed at least twice, and the results of independent analyses were highly reproducible (Supplementary Fig. S1). We found that the mean level of *LINE-1* methylation in the 106 GIST specimens was 57.3 ± 9.3% (mean ± SD; range, 27.9-74.1%), and that the level was slightly lower in female patients than male patients, although the difference was not statistically significant (male, 58.8%; female, 55.9%; P = 0.055). We found no correlation between tumor location and *LINE-1* methylation (stomach, 58.6%; small intestine, 54.4%; esophagus, 51.9%; omentum, 57.7%; colon, 56.2%; P = 0.4136), and there was no correlation between age and *LINE-1* methylation (<60 years, 56.5%; 61-70 years, 58.8%; >71 years, 57.9%; P = 0.687).

We then compared *LINE-1* methylation with risk classification. The single very low-risk GIST specimen showed a high level of *LINE-1* methylation (74.1%). Low-risk (n = 23) and intermediate-risk (n = 19) GISTs showed similar levels of *LINE-1* methylation (61.3% versus 60.8%). By contrast, high-risk GISTs (n = 42) exhibited a significantly lower level of *LINE-1* methylation (53.2%) than GISTs in the other risk groups (Fig. 1A). Using that information, we stratified the tumors according to their level of *LINE-1* methylation, which was then correlated with the risk categories. After adjusting for age and gender, the lowest level of *LINE-1* methylation (<54.9%) was significantly associated with the high-risk category [OR, 7.5; 95%

Table 2. Correlation between *LINE-1* methylation and the GIST risk category

LINE-1 methylation (%)	All samples (N = 76)	High-risk (n = 36)	Very low-, low-, or intermediate-risk (n = 40)	P	OR* (95% CI)
>68.0	13	4	9		1.0
61.4-67.9	14	4	10	0.976	1.0 (0.2-5.5)
54.9-61.3	22	8	14	0.638	1.4 (0.3-6.5)
<54.9	27	20	7	0.009	7.5 (1.6-34.0)
				P trend < 0.001	

*Age- and gender-adjusted OR.

Published OnlineFirst October 26, 2010; DOI:10.1158/1078-0432.CCR-10-0581

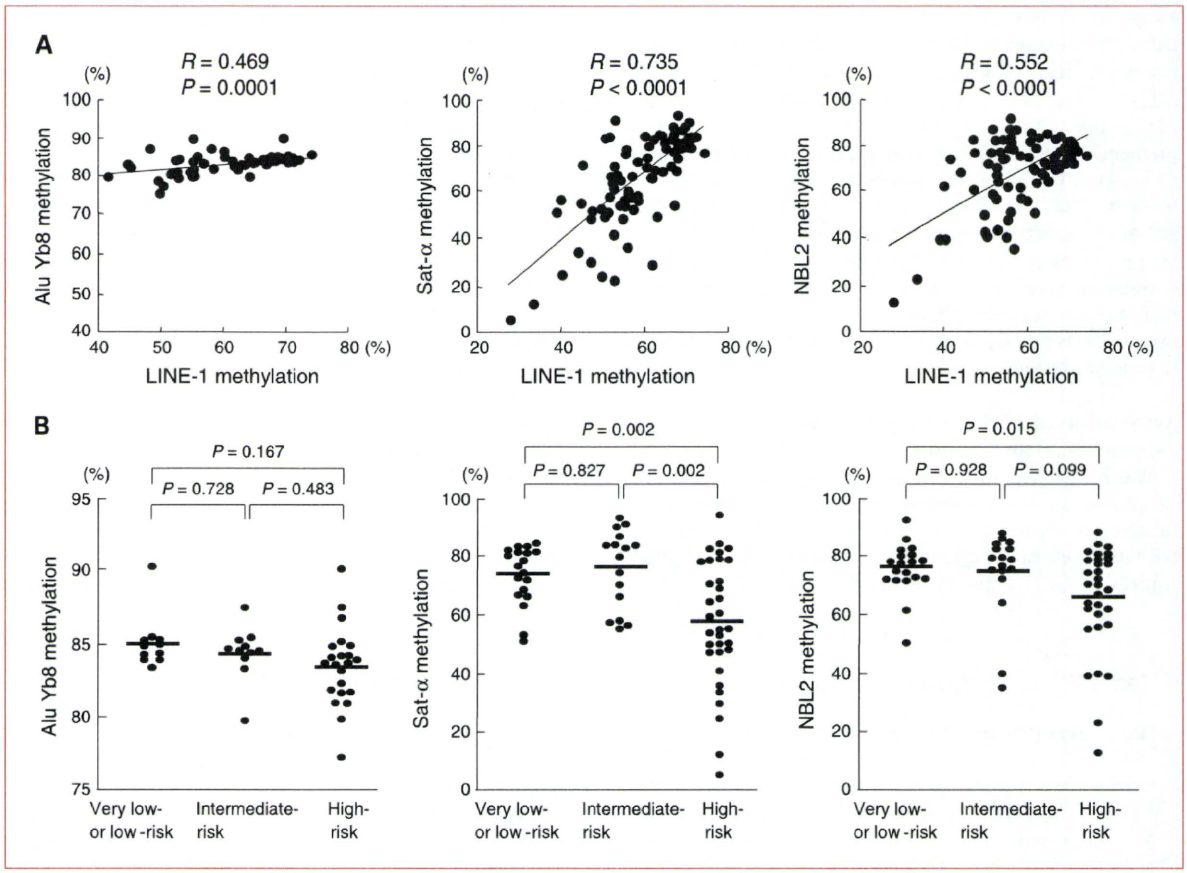

Fig. 2. Analysis of the methylation of different repetitive sequences in GISTs. A, methylation levels in three different repetitive sequences (*Alu Yb8*, *Sat-α*, and *NBL2*) were analyzed and correlated with *LINE-1* methylation. The Pearson correlation coefficients and *P* values are shown. B, comparison of the methylation of repetitive sequences among low-, intermediate-, and high-risk GISTs. Filled circles represent average methylation (%) at multiple CpG sites.

confidence interval (CI), 1.6-34.0; Table 2]. Moreover, bivariate correlation analysis revealed an inverse correlation between *LINE-1* methylation levels and tumor size (Fig. 1B). Among the high-risk GIST patients, *LINE-1* methylation was slightly lower in individuals with incidences of metastasis than in those without metastasis (50.0% versus 54.8%), although the difference was not statistically significant (Fig. 1C). However, when we divided high-risk GIST patients into two groups according to *LINE-1* methylation and did logistic regression analysis, we found that GISTs with lower *LINE-1* methylation (<55%) were significantly associated with incidences of metastasis (OR, 9.5; 95% CI, 1.5-61.2; Supplementary Table S1). These results suggest that *LINE-1* hypomethylation is strongly associated with greater risk and aggressiveness of GISTs.

Hypomethylation of other repetitive DNA elements in GIST

Previous studies showed that Alu elements and other repetitive sequences are also hypomethylated in human malignancies (15–20). We therefore carried out bisulfite pyrosequencing of *Alu Yb8* and two other tandem repeats, *Sat-α* and *NBL2*, which are reportedly hypomethylated in cancer (15, 20). We found a moderate correlation between *LINE-1* methylation and *Alu Yb8* methylation (Fig. 2A); however, levels of *Alu Yb8* methylation did not significantly correlate with risk grade (Fig. 2B). By contrast, *LINE-1* methylation strongly correlated with *Sat-α* and *NBL2* methylation (Fig. 2A). High-risk GISTs showed significantly lower levels of *Sat-α* methylation than low-risk (57.9% versus 73.9%) or intermediate-risk GISTs (57.9% versus 76.3%; Fig. 2B), and significantly lower levels of *NBL2* methylation than low-risk GISTs (65.1% versus 75.5%; Fig. 2B).

Analysis of CpG island hypermethylation of tumor-related genes

Because it was previously reported that CpG island methylation correlates with GIST malignancy (21), we next assessed the methylation levels of the CpG islands of several well-characterized tumor suppressor and tumor-related genes in the GIST specimens. Using MethyLight

Published OnlineFirst October 26, 2010; DOI:10.1158/1078-0432.CCR-10-0581

assays, we analyzed nine genes frequently methylated in gastrointestinal cancers. Unexpectedly, methylation of these genes was relatively infrequent in GISTs (*CDH1*, 12.2%; *MLH1*, 9.8%; *SFRP1*, 1.2%; *SFRP2*, 11.0%; *CHFR*, 9.8%; *APC*, 6.1%; *CDKN2A*, 0%; *RASSF1A*, 0%; *RASSF2*, 0%; Supplementary Table S2). Interestingly, however, *CDH1* tended to be methylated more frequently in higher-risk GISTs, whereas *MLH1* tended to be methylated less frequently, although these correlations were not statistically significant (Supplementary Table S2). We failed to find any significant correlation between methylation of other genes and clinicopathologic features. There was also no significant correlation between CpG island methylation and *LINE-1* hypomethylation.

Association of *LINE-1* methylation with chromosomal aberrations

The biological meaning of global hypomethylation in tumors is not yet fully understood, but it is thought to be associated with chromosomal instability (5). Consistent with that idea, earlier cytogenetic, fluorescence *in situ* hybridization, and CGH studies revealed frequent chromosomal imbalances in GISTs (28–32). This prompted us to ask whether *LINE-1* hypomethylation in GISTs is associated with chromosomal gain or loss. We addressed that question by carrying out an array CGH analysis using 25 freshly frozen GIST specimens using an Agilent 105K oligonucleotide microarray.

We found that the average number of chromosomal aberrations for a given tumor was 28.5 (range, 5-62), and genomic losses were much more common than gains. Consistent with previous CGH and array CGH studies of GIST (28–32), we observed frequent genomic losses at 14q (92%), 22q (68%), 15q (64%), and 1p (60%; Table 3; Supplementary Fig. S2; Supplementary Table S3). Total or partial losses at 14q were the most frequent chromosomal aberration (23 of 25; 92%), and 17 GISTs showed a total loss of chromosome 14. Total or partial losses of 22q were also frequently detected (17 of 25; 68%), and 11 tumors showed a loss of the whole chromosome. Losses at 1p were detected in 15 of 25 tumors (60%), and losses were generally more frequent in intestinal GISTs than in gastric ones (Table 3). Losses at 15q were often associated with 1p loss, which is consistent with an earlier observation

Table 3. Summary of the frequent chromosomal losses detected using array CGH

No.	Age/gender	Location	Risk	L-1 (%)	Chromosomal losses							
					1p	3q	4q	9p	13q	14q	15q	22q
1	67/M	Stomach	Low	71.2		Yes	Yes			Yes*	Yes	Yes
2	65/M	Stomach	Inter.	71.1			Yes	Yes		Yes*		Yes
3	64/F	Stomach	Low	70.1					Yes	Yes	Yes*	
4	50/M	Stomach	Low	69.5	Yes	Yes	Yes			Yes		
5	27/F	Stomach	Inter.	68.8		Yes	Yes			Yes*		Yes
6	68/F	Stomach	Low	68.6		Yes	Yes			Yes*		
7	61/M	Small intestine	Low	67.6	Yes*	Yes	Yes			Yes*	Yes	Yes*
8	62/F	Stomach	Low	64.7	Yes	Yes	Yes			Yes*	Yes	
9	65/F	Stomach	Low	64.0		Yes	Yes			Yes*		Yes
10	25/F	Small intestine	Inter.	60.5	Yes*	Yes	Yes		Yes	Yes*	Yes*	
11	70/M	Stomach	Inter.	60.3		Yes				Yes*		Yes
12	53/F	Stomach	High	58.3		Yes	Yes			Yes		
13	56/M	Small intestine	Inter.	56.6	Yes	Yes	Yes	Yes			Yes*	Yes*
14	65/M	Stomach	High	56.0			Yes			Yes	Yes	
15	37/M	Small intestine	High	55.2	Yes*	Yes	Yes	Yes		Yes	Yes*	Yes*
16	63/M	Stomach	Inter.	55.0	Yes	Yes	Yes	Yes		Yes*	Yes	Yes*
17	73/F	Stomach	NA	52.7		Yes	Yes	Yes		Yes		
18	68/F	Small intestine	High	52.5	Yes*	Yes	Yes	Yes	Yes*	Yes*	Yes*	Yes*
19	62/M	Small intestine	NA	51.5	Yes*	Yes	Yes				Yes*	Yes*
20	57/M	Small intestine	High	50.3	Yes*		Yes	Yes*		Yes*	Yes*	Yes*
21	49/M	Stomach	NA	49.7	Yes	Yes		Yes*	Yes	Yes*		Yes*
22	68/M	Small intestine	NA	49.5	Yes*	Yes	Yes	Yes*	Yes*	Yes*	Yes*	Yes*
23	73/F	Stomach	High	47.0	Yes			Yes		Yes*	Yes	Yes
24	87/M	Small intestine	High	44.0	Yes*	Yes	Yes		Yes*	Yes*	Yes*	Yes*
25	68/F	Stomach	High	33.4	Yes		Yes	Yes*	Yes	Yes*	Yes	Yes*

Abbreviations: L-1, *LINE-1* methylation; Inter., intermediate; NA, not available.
*Loss of the entire p- or q-arm of the chromosome.

Published OnlineFirst October 26, 2010; DOI:10.1158/1078-0432.CCR-10-0581

(Table 3; ref. 31). Partial losses at 3q were also frequently detected (19 of 25; 76%), and a minimal common overlapping region was identified at 3q26.1, although this region contains no annotated genes (Supplementary Table S3). In addition, losses at 4q13.2, the locus of *UGT2B17/UGT2B28*, were detected in 20 of 25 tumors (80%). Losses at 9p were found in 11 of 25 (44%) GISTs, and 4 tumors showed a loss of the whole p-arm. Among seven tumors with partial 9p losses, four showed a loss at 9p21, the locus of *CDKN2A/CDKN2B*.

Losses at 3q, 4q, 14q, and 22q were found to be equally distributed in tumors with all levels of *LINE-1* methylation (Table 3). By contrast, many other chromosomal aberrations correlated with *LINE-1* hypomethylation (Table 3; Fig. 3A). For example, GISTs with losses at 1p showed significantly lower *LINE-1* methylation than those without 1p loss (53.8% versus 64.1%; $P = 0.007$). *LINE-1* methylation was also much lower in tumors with loss at 9p than in those without that loss (52.1% versus 62.5%; $P = 0.005$). Bivariate correlation analysis revealed a significant inverse correlation between levels of *LINE-1* methylation and the total number of chromosomal aberrations, including both losses and gains (Fig. 3B). These results suggest a significant relationship between *LINE-1* hypomethylation and DNA copy number abnormalities in GIST.

Discussion

Although several studies have shown that genetic abnormalities, including various mutations and chromosomal imbalances, are significantly involved in the development of GISTs, little is known about the role played by epigenetic alterations in these tumors. To date, there had been only a few reports of CpG island methylation in GISTs (21–24), and levels of global DNA methylation had not yet been analyzed. In the present study, however, we found that levels of methylation of *LINE-1* and other repetitive elements are reduced in GISTs. It has been known for decades that global hypomethylation is a common feature of human cancer (33, 34), and in recent years, hypomethylation has been studied in various human malignancies using *LINE-1* and other repetitive sequences as surrogates

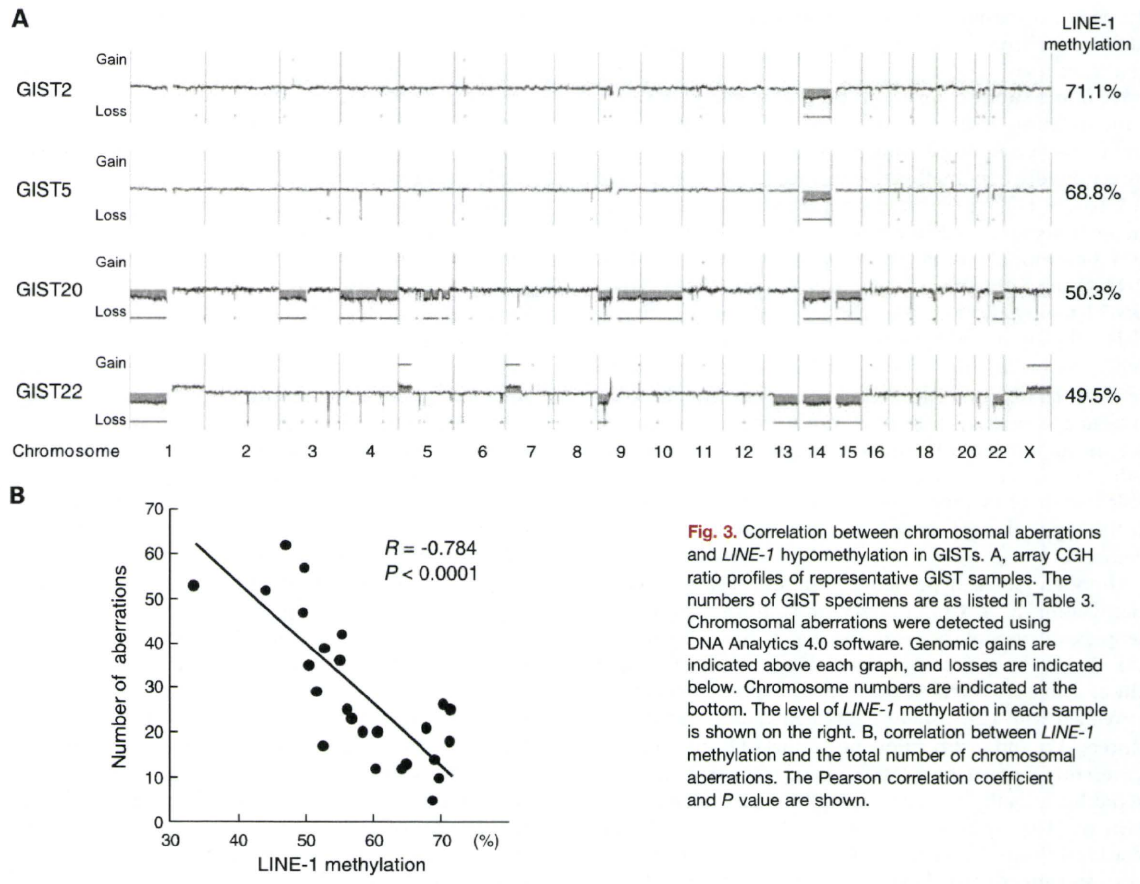

Fig. 3. Correlation between chromosomal aberrations and *LINE-1* hypomethylation in GISTs. A, array CGH ratio profiles of representative GIST samples. The numbers of GIST specimens are as listed in Table 3. Chromosomal aberrations were detected using DNA Analytics 4.0 software. Genomic gains are indicated above each graph, and losses are indicated below. Chromosome numbers are indicated at the bottom. The level of *LINE-1* methylation in each sample is shown on the right. B, correlation between *LINE-1* methylation and the total number of chromosomal aberrations. The Pearson correlation coefficient and *P* value are shown.

Published OnlineFirst October 26, 2010; DOI:10.1158/1078-0432.CCR-10-0581

(9–20). Our results confirm that GISTs exhibit a pattern of hypomethylation that is similar to those exhibited by many other human tumors.

We found that *LINE-1* hypomethylation is strongly associated with the aggressiveness of GISTs. Levels of *LINE-1* methylation were significantly lower in high-risk GISTs than in low- or intermediate-risk tumors. In addition, levels of *LINE-1* methylation inversely correlated with tumor size and mitotic counts. These results are consistent with earlier observations that a reduction in global methylcytosine content is associated with malignant potential in cancer, and that it is especially prevalent in metastatic tumors (34). *LINE-1* hypomethylation is also reportedly associated with poor prognosis in prostate (17), colon (35), and ovarian (36) cancers and in chronic myeloid leukemia (11). In normal cells, DNA methylation plays important roles in X-chromosome inactivation, genomic imprinting, and repression of repetitive elements, such as retrotransposons and endogenous retroviruses. Thus, hypomethylation may associate with tumor malignancy through a variety of mechanisms. For example, global hypomethylation is associated with genomic instability (37–40), which may confer a poor prognosis. Hypomethylation can also lead to activation of proto-oncogenes, endogenous retroviruses, or transposable elements, and such transcriptional dysregulation could affect tumor aggressiveness.

We found strong correlations between the level of LINE-1 methylation and methylation of other repetitive elements. *Sat-α* and *NBL2*, which are tandem DNA repeats, are reportedly hypomethylated in various human cancers (15, 16, 20, 41). We observed that methylation of these elements is also reduced in high-risk GISTs, which suggests that a common mechanism may induce and maintain DNA hypomethylation in tumors. On the other hand, *LINE-1* methylation correlated only moderately with *Alu Yb8* methylation, and hypomethylation of *Alu Yb8* was limited, even in high-risk GISTs. Similar modest correlation between *LINE-1* and Alu methylation was also observed in head and neck squamous cell carcinomas and neuroendocrine tumors (18, 42). This lower correlation may simply reflect a difference in assay sensitivity, although it is possible that there are functional and/or biological differences in the regulation of these two types of repetitive DNA elements.

Although global hypomethylation and regional hypermethylation of 5′ CpG islands are common features of neoplasias, the link between the two remains controversial. Recent studies using methylation of *LINE-1* and/or Alu as a marker revealed that global hypomethylation is correlated with CpG island hypermethylation in prostate cancers (17) and neuroendocrine tumors (42). In addition, we recently showed that *LINE-1* hypomethylation and CpG island hypermethylation are tightly linked in enlarged fold gastritis (14). By contrast, others did not find a similar relationship in Wilm's tumor (41), colon cancer (43), or ovarian cancer (16). Recent studies also revealed that *LINE-1* hypomethylation is inversely correlated with microsatellite instability and/or the CpG island methylator phenotype in colon cancer, suggesting that CpG island hypermethylation and global hypomethylation may reflect different tumor progression pathways (12, 13). In the present study, we failed to find a significant correlation between 5′ CpG island hypermethylation of tumor-related genes and global hypomethylation. However, this may reflect a bias toward selection of genes frequently methylated in tumors of epithelial origin, as GISTs may exhibit methylation of a different spectrum of genes.

House et al. (21) reported that hypermethylation of *CDH1* (*E-cadherin*) is positively correlated with GISTs having malignant histologic features (mitotic rate, tumor size, and necrosis) and a poor prognosis. In addition, the presence of *CDH1* methylation and the absence of *MLH1* methylation correlated with early tumor recurrence. By contrast, Saito et al. (24) reported that CpG island hypermethylation, including that of *MLH1* and *CDH1*, was frequently detected in GISTs, irrespective of their malignancy. In the present study, we found tendencies for *CDH1* methylation to occur more frequently and *MLH1* methylation to occur less frequently in higher-risk GISTs, although these correlations were not statistically significant. We also noticed that the frequencies of CpG island methylation were lower than those reported previously (21, 24). This could reflect differences in the primer sequences used in our study, but the actual reason for the discrepancy is not clear. As mentioned above, GISTs may exhibit hypermethylation of a different spectrum of genes, and further study will be needed to clarify the role of CpG island methylation in GISTs.

Global hypomethylation is strongly implicated in chromosomal instability. A study using $Nf1^{+/-}$ $p53^{+/-}$ mice has shown that introduction of a hypomorphic *Dnmt1* allele causes DNA hypomethylation that leads to significant increases in the loss of heterozygosity rate and tumor development (37). Another study has shown that hypomethylation in $Apc^{Min/+}$ mice leads to increases in microadenoma formation through loss of heterozygosity at the *Apc* locus (38). Global hypomethylation also correlates with chromosomal instability and copy number changes in human cancers (18, 19, 39, 40). Thus, to assess the potential implication of *LINE-1* hypomethylation in genomic instability in GISTs, we carried out an array CGH analysis and correlated hypomethylation with chromosomal imbalances. The results of this analysis are largely consistent with previously reported cytogenetic, CGH, and array CGH analyses of GISTs (28–32). In general, losses were more common than gains, and genomic losses frequently affected 1p, 14q, 15q, and 22q. In addition, we found losses at 3q26.1 and 4q13.2, the locus of *UGT2B17*/*UGT2B28*, in the majority of tumors tested. UGT2B17, which is a member of the UDP-glucuronosyltransferases (UGT) family, has been implicated in the metabolism of androgens, and a deletion polymorphism in *UGT2B17* is reportedly associated with the risk of prostate cancer (44), although its functional role in GISTs remains to be clarified.

Published OnlineFirst October 26, 2010; DOI:10.1158/1078-0432.CCR-10-0581

Although the most frequent aberrations (e.g., losses of 14q and 22q) were equally distributed among GISTs with all levels of *LINE-1* methylation, we found a significant correlation between many other chromosomal aberrations and DNA hypomethylation. For instance, tumors with losses at 1p or 9p showed significantly lower *LINE-1* methylation. Notably, these results are consistent with previous findings that losses at 14q and 22q are early changes in GIST development, whereas losses at 1p and 9p are associated with malignancy and poor prognosis (28–31). Moreover, total numbers of chromosomal aberrations are highly correlated with *LINE-1* hypomethylation. It thus seems that *LINE-1* hypomethylation may play an important role in inducing chromosomal aberrations and increasing the aggressiveness of GISTs. Currently, however, we have no functional evidence of a causal relationship between hypomethylation and the genomic instability of GISTs, and further studies will be required to clarify the underlying molecular mechanism.

In summary, we found that hypomethylation of repetitive elements is associated with high-risk GISTs. We also provide further evidence that *LINE-1* hypomethylation is strongly associated with chromosomal aberrations. Although the cause of DNA hypomethylation in GISTs remains unclear, *LINE-1* methylation could be a useful marker for predicting the risk and prognosis of the disease.

Disclosure of Potential Conflicts of Interest

No potential conflicts of interest were disclosed.

Acknowledgments

We thank Dr. William F. Goldman for editing the manuscript and M. Ashida for technical assistance.

Grant Support

Grants-in-Aid for Scientific Research on Priority Areas (M. Toyota and K. Imai), Program for developing the supporting system for upgrading the education and research from the Ministry of Education, Culture, Sports, Science, and Technology (Y. Shinomura and M. Toyota), A3 foresight program from the Japan Society for Promotion of Science (H. Suzuki), Grants-in-Aid for Scientific Research (B) from the Japan Society for Promotion of Science (Y. Shinomura), Grants-in-Aid for Scientific Research (S) from the Japan Society for Promotion of Science (K. Imai), a Grant-in-Aid for the Third-term Comprehensive 10-year Strategy for Cancer Control (M. Toyota), and a Grant-in-Aid for Cancer Research from the Ministry of Health, Labor, and Welfare, Japan (M. Toyota).

The costs of publication of this article were defrayed in part by the payment of page charges. This article must therefore be hereby marked *advertisement* in accordance with 18 U.S.C. Section 1734 solely to indicate this fact.

Received 03/06/2010; revised 06/08/2010; accepted 06/20/2010; published OnlineFirst 10/26/2010.

References

1. Shinomura Y, Kinoshita K, Tsutsui S, et al. Pathophysiology, diagnosis, and treatment of gastrointestinal stromal tumors. J Gastroenterol 2005;40:775–80.
2. Rubin BP, Heinrich MC, Corless CL. Gastrointestinal stromal tumour. Lancet 2007;369:1731–41.
3. Yang J, Du X, Lazar AJ, et al. Genetic aberrations of gastrointestinal stromal tumors. Cancer 2008;113:1532–43.
4. Fletcher CD, Berman JJ, Corless C, et al. Diagnosis of gastrointestinal stromal tumors: a consensus approach. Hum Pathol 2002;33:459–65.
5. Jones PA, Baylin SB. The fundamental role of epigenetic events in cancer. Nat Rev Genet 2002;3:415–28.
6. Suzuki H, Tokino T, Shinomura Y, Imai K, Toyota M. DNA methylation and cancer pathways in gastrointestinal tumors. Pharmacogenomics 2008;9:1917–28.
7. Cordaux R, Batzer MA. The impact of retrotransposons on human genome evolution. Nat Rev Genet 2009;10:691–703.
8. Yang AS, Estécio MR, Doshi K, Kondo Y, Tajara EH, Issa JP. A simple method for estimating global DNA methylation using bisulfite PCR of repetitive DNA elements. Nucleic Acids Res 2004;32:e38.
9. Takai D, Yagi Y, Habib N, Sugimura T, Ushijima T. Hypomethylation of LINE1 retrotransposon in human hepatocellular carcinomas, but not in surrounding liver cirrhosis. Jpn J Clin Oncol 2000;30:306–9.
10. Chalitchagorn K, Shuangshoti S, Hourpai N, et al. Distinctive pattern of LINE-1 methylation level in normal tissues and the association with carcinogenesis. Oncogene 2004;23:8841–6.
11. Roman-Gomez J, Jimenez-Velasco A, Agirre X, et al. Promoter hypomethylation of the LINE-1 retrotransposable elements activates sense/antisense transcription and marks the progression of chronic myeloid leukemia. Oncogene 2005;24:7213–23.
12. Estécio MR, Gharibyan V, Shen L, et al. LINE-1 hypomethylation in cancer is highly variable and inversely correlated with microsatellite instability. PLoS One 2007;2:e399.
13. Ogino S, Kawasaki T, Nosho K, et al. LINE-1 hypomethylation is inversely associated with microsatellite instability and CpG island methylator phenotype in colorectal cancer. Int J Cancer 2008;122:2767–73.
14. Yamamoto E, Toyota M, Suzuki H, et al. LINE-1 hypomethylation is associated with increased CpG island methylation in *Helicobacter pylori*-related enlarged-fold gastritis. Cancer Epidemiol Biomarkers Prev 2008;17:2555–64.
15. Itano O, Ueda M, Kikuchi K, et al. Correlation of postoperative recurrence in hepatocellular carcinoma with demethylation of repetitive sequences. Oncogene 2002;21:789–97.
16. Ehrlich M, Woods CB, Yu MC, et al. Quantitative analysis of associations between DNA hypermethylation, hypomethylation, and DNMT RNA levels in ovarian tumors. Oncogene 2006;25:2636–45.
17. Cho NY, Kim BH, Choi M, et al. Hypermethylation of CpG island loci and hypomethylation of LINE-1 and Alu repeats in prostate adenocarcinoma and their relationship to clinicopathological features. J Pathol 2007;211:269–77.
18. Richards KL, Zhang B, Baggerly KA, et al. Genome-wide hypomethylation in head and neck cancer is more pronounced in HPV-negative tumors and is associated with genomic instability. PLoS One 2009;4:e4941.
19. Daskalos A, Nikolaidis G, Xinarianos G, et al. Hypomethylation of retrotransposable elements correlates with genomic instability in non-small cell lung cancer. Int J Cancer 2009;124:81–7.
20. Choi SH, Worswick S, Byun HM, et al. Changes in DNA methylation of tandem DNA repeats are different from interspersed repeats in cancer. Int J Cancer 2009;125:723–9.
21. House MG, Guo M, Efron DT, et al. Tumor suppressor gene hypermethylation as a predictor of gastric stromal tumor behavior. J Gastrointest Surg 2003;7:1004–14.
22. Ricci R, Arena V, Castri F, et al. Role of p16/INK4a in gastrointestinal stromal tumor progression. Am J Clin Pathol 2004;122:35–43.
23. Perrone F, Tamborini E, Dagrada GP, et al. 9p21 locus analysis in high-risk gastrointestinal stromal tumors characterized for c-kit and platelet-derived growth factor receptor α gene alterations. Cancer 2005;104:159–69.
24. Saito K, Sakurai S, Sano T, et al. Aberrant methylation status of

Published OnlineFirst October 26, 2010; DOI:10.1158/1078-0432.CCR-10-0581

known methylation-sensitive CpG islands in gastrointestinal stromal tumors without any correlation to the state of c-kit and PDGFRA gene mutations and their malignancy. Cancer Sci 2008;99:253–9.
25. Weisenberger DJ, Campan M, Long TI, et al. Analysis of repetitive element DNA methylation by MethyLight. Nucleic Acids Res 2005; 33:6823–36.
26. Weisenberger DJ, Siegmund KD, Campan M, et al. CpG island methylator phenotype underlies sporadic microsatellite instability and is tightly associated with BRAF mutation in colorectal cancer. Nat Genet 2006;38:787–93.
27. Nosho K, Yamamoto H, Takahashi T, et al. Genetic and epigenetic profiling in early colorectal tumors and prediction of invasive potential in pT1 (early invasive) colorectal cancers. Carcinogenesis 2007; 28:1364–70.
28. Kim NG, Kim JJ, Ahn JY, et al. Putative chromosomal deletions on 9P, 9Q and 22Q occur preferentially in malignant gastrointestinal stromal tumors. Int J Cancer 2000;85:633–8.
29. El-Rifai W, Sarlomo-Rikala M, Andersson LC, et al. DNA sequence copy number changes in gastrointestinal stromal tumors: tumor progression and prognostic significance. Cancer Res 2000;60: 3899–903.
30. Gunawan B, Bergmann F, Höer J, et al. Biological and clinical significance of cytogenetic abnormalities in low-risk and high-risk gastrointestinal stromal tumors. Hum Pathol 2002;33:316–21.
31. Wozniak A, Sciot R, Guillou L, et al. Array CGH analysis in primary gastrointestinal stromal tumors: cytogenetic profile correlates with anatomic site and tumor aggressiveness, irrespective of mutational status. Genes Chromosomes Cancer 2007;46:261–76.
32. Assämäki R, Sarlomo-Rikala M, Lopez-Guerrero JA, et al. Array comparative genomic hybridization analysis of chromosomal imbalances and their target genes in gastrointestinal stromal tumors. Genes Chromosomes Cancer 2007;46:564–76.
33. Feinberg AP, Vogelstein B. Hypomethylation distinguishes genes of some human cancers from their normal counterparts. Nature 1983; 301:89–92.
34. Gama-Sosa MA, Slagel VA, Trewyn RW, et al. The 5-methylcytosine content of DNA from human tumors. Nucleic Acids Res 1983;11: 6883–94.
35. Ogino S, Nosho K, Kirkner GJ, et al. A cohort study of tumoral LINE-1 hypomethylation and prognosis in colon cancer. J Natl Cancer Inst 2008;100:1734–8.
36. Pattamadilok J, Huapai N, Rattanatanyong P, et al. LINE-1 hypomethylation level as a potential prognostic factor for epithelial ovarian cancer. Int J Gynecol Cancer 2008;18:711–7.
37. Eden A, Gaudet F, Waghmare A, Jaenisch R. Chromosomal instability and tumors promoted by DNA hypomethylation. Science 2003;300:455.
38. Yamada Y, Jackson-Grusby L, Linhart H, et al. Opposing effects of DNA hypomethylation on intestinal and liver carcinogenesis. Proc Natl Acad Sci U S A 2005;102:13580–5.
39. Karpf AR, Matsui S. Genetic disruption of cytosine DNA methyltransferase enzymes induces chromosomal instability in human cancer cells. Cancer Res 2005;65:8635–9.
40. Rodriguez J, Frigola J, Vendrell E, et al. Chromosomal instability correlates with genome-wide DNA demethylation in human primary colorectal cancers. Cancer Res 2006;66:8462–8.
41. Ehrlich M, Jiang G, Fiala E, et al. Hypomethylation and hypermethylation of DNA in Wilms tumors. Oncogene 2002;21: 6694–702.
42. Choi IS, Estecio MR, Nagano Y, et al. Hypomethylation of LINE-1 and Alu in well-differentiated neuroendocrine tumors (pancreatic endocrine tumors and carcinoid tumors). Mod Pathol 2007;20: 802–10.
43. Iacopetta B, Grieu F, Phillips M, et al. Methylation levels of LINE-1 repeats and CpG island loci are inversely related in normal colonic mucosa. Cancer Sci 2007;98:1454–60.
44. Park J, Chen L, Ratnashinge L, et al. Deletion polymorphism of UDP-glucuronosyltransferase 2B17 and risk of prostate cancer in African American and Caucasian men. Cancer Epidemiol Biomarkers Prev 2006;15:1473–8.

Chemico-Biological Interactions 184 (2010) 423–430

Contents lists available at ScienceDirect

Chemico-Biological Interactions

journal homepage: www.elsevier.com/locate/chembioint

Genetic ablation of *Tnfα* demonstrates no detectable suppressive effect on inflammation-related mouse colon tumorigenesis

Hiroyasu Sakai[a,b], Yasuhiro Yamada[a,c,d,*], Masahito Shimizu[b], Kuniaki Saito[e], Hisataka Moriwaki[b], Akira Hara[a]

[a] Department of Tumor Pathology, Gifu University Graduate School of Medicine, 1-1 Yanagido, Gifu 501-1194, Japan
[b] Department of Medicine, Gifu University Graduate School of Medicine, 1-1 Yanagido, Gifu 501-1194, Japan
[c] PRESTO, Japan Science and Technology Agency, 4-1-8 Honcho Kawaguchi, Saitama, Japan
[d] Center for iPS Cell Research and Application (CiRA), Institute for Integrated Cell-material Sciences, Kyoto University, Kyoto 606-8507, Japan
[e] Human Health Science, Graduate School of Medicine and Faculty of Medicine, Kyoto University, 53 Kawahara-cho, Shogoin, Sakyo, Kyoto 606-8507, Japan

ARTICLE INFO

Article history:
Received 16 December 2009
Received in revised form 4 January 2010
Accepted 6 January 2010
Available online 14 January 2010

Keywords:
Tnfα
Inflammation-related colorectal cancer
Mouse

ABSTRACT

Colorectal cancer (CRC) is one of the most serious complications of inflammatory bowel disease. Tumor necrosis factor-α (Tnfα) is a major mediator of inflammation and there is increasing evidence that Tnfα/Tnf-receptor-1 (Tnfr1) signaling may act as an endogenous tumor promoter for colon carcinogenesis. In fact, a previous study revealed that mice lacking *Tnfr1* develop significantly fewer colonic tumors in the inflammation-related CRC model. In addition, antibodies against Tnfα have been shown to inhibit the development of inflammation-related CRC. In the present study, *Apc* Min/+; *Tnfα* −/− mice were treated with 2% dextran sodium sulfate (DSS) and the tumor development was compared with *Apc* Min/+; *Tnfα* +/+ control mice in order to investigate the role of Tnfα by itself in the inflammation-related CRC. Surprisingly, there were no detectable differences in either the severity of colonic inflammation or the expression of DSS-induced chemokines and cytokines (*Ccl2*, *Cxcl1*, *Tnfβ*, *Il1β*, *Il6*, and *Cox-2*) that relate to the colonic inflammation and tumorigenesis between these two groups. Furthermore, the genetic ablation of *Tnfα* did not suppress the colon tumorigenesis in comparison to the wild-type mice. Our observations suggest that intricate inflammatory responses promote the inflammation-related mouse colon tumorigenesis.

1. Introduction

The link between carcinogenesis and chronic inflammation has been recognized for certain types of cancer, including colorectal cancer (CRC) [1]. CRC is one of the serious complications of inflammatory bowel disease (IBD), including ulcerative colitis and Crohn's disease [1,2]. Although previous studies have demonstrated that the link between inflammation and CRC offers a possible strategy to prevent CRC, the underlying molecular processes involved in this interaction still remain poorly understood. Tumor necrosis factor-α (Tnfα) is a key cytokine involved in inflammation, immunity and cellular organization [3]. It was first isolated from the serum of mice infected with *Bacillus-Calmette–Guerin* treated with endotoxin, and shown to replicate the ability of endotoxin to induce haemorrhagic tumor necrosis [4]. Accordingly, it was originally utilized for the treatment of patients with advanced solid tumors [5]. In contrast, recent evidence indicates that Tnfα may act as an endogenous tumor promoter in several tumor tissues. Direct evidence for the involvement of Tnfα in malignancy came from observations that a genetic disruption of the *Tnfα* gene could significantly attenuate chemically induced skin tumor formation [6–8]. In addition, *Tnf-receptor-1* (*Tnfr1*) deficient mice had reduced oval cell (the putative hepatic stem cell) proliferation during the pre-neoplastic phase of liver carcinogenesis, correlating with fewer liver tumors than wild-type mice [9]. It has therefore been suggested that the Tnfα/Tnfr1 signaling pathway may play an important role in tumor promotion.

The predominant expression of Tnfα in colorectal cancer is observed within tumor-associated macrophages [10]. A previous study reported that Tnfα and Tnfr1 protein are expressed mainly in the infiltrating cells, such as macrophages and neutrophils which are derived from myeloid cells in inflamed colon tissue [11]. These infiltrating cells also express Cox-2 protein which is often up-regulated in colon carcinoma tissues and functionally promotes intestinal tumorigenesis [12]. Furthermore, Greten et al. reported that depleting *Ikkβ* in myeloid cells reduced the expression of pro-

Abbreviations: Tnfα, tumor necrosis factor-α; IBD, inflammatory bowel disease; Tnfr1, tumor necrosis factor-receptor-1; CRC, colorectal cancer; DSS, dextran sodium sulfate; Apc, adenomatous polyposis coli; Min, multiple intestinal neoplasia.

* Corresponding author at: Department of Tumor Pathology, Gifu University Graduate School of Medicine, 1-1 Yanagido, Gifu 501-1194, Japan. Tel.: +81 58 230 6225; fax: +81 58 230 6226.
E-mail addresses: y-yamada@cira.kyoto-u.ac.jp, y-yamada@gifu-u.ac.jp (Y. Yamada).

0009-2797/$ – see front matter © 2010 Elsevier Ireland Ltd. All rights reserved.
doi:10.1016/j.cbi.2010.01.014

inflammatory factor genes encoding Tnfα, Il1β, Il6, Kc, Cox-2 and Mmp-9 in the colon, followed by a suppression of colorectal tumor development in inflammation-related colon tumorigenesis [13].

It is noteworthy that the absence of *Tnfr*1 significantly reduces the DSS-induced infiltration of Cox-2-expressing inflammatory cells, thus leading to a reduced incidence of colonic tumors [11]. Moreover, Tnfα can significantly increase Nf-kb activation in various cell types after binding to either Tnfr1 or Tnf-receptor-2 (Tnfr2) [14]. Therefore, it has been thought that endogenous Tnfα may activate Nf-kb signaling in inflammatory cells by interacting with Tnfr1 in an autocrine/paracrine manner and activated Nf-kb increases the expression of pro-inflammatory factors, which could thus lead to the promotion of colorectal tumorigenesis. Given the fact that Tnfr1 signaling is associated with tumorigenesis in the colon, Tnfα itself might be a therapeutic target for the inflammation-related mouse colon tumorigenesis. Indeed, previous studies demonstrated that antibodies against Tnfα inhibit the development of inflammation-related CRC [15].

Several animal models of experimental colitis have been developed for investigating the pathogenesis of IBD and IBD-related CRC and these are often used to evaluate new treatments for IBD [16]. Chemically induced models of intestinal inflammation, such as the dextran sodium sulfate (DSS)-induced model and the trinitrobenzene sulfonic acid (TNBS)-induced model, are the most generally used IBD animal models because the onset of inflammation is immediate and the procedure is relatively straightforward [17,18]. In contrast to the involvement of CD4+ T cells in TNBS-induced colitis, macrophages have been shown to play a central role in DSS-induced colitis [18,19]. Importantly, once *Apc* Min/+ mice, which harbor a germ line mutation in the *Apc* gene, are exposed to DSS, colitis markedly accelerates the development of dysplasia and cancer in the colon of *Apc* Min/+ mice [20]. Therefore, DSS-treated *Apc* Min/+ mouse can be useful for the investigation of inflammation-related colorectal tumorigenesis. The current study examined the effects of the genetic ablation of *Tnfα* on colon tumorigenesis using *Apc* Min/+; *Tnfα* −/− compound mutant mice exposed to DSS in order to determine whether Tnfα by itself could be a target for the prevention/treatment of inflammation-related colon tumorigenesis.

2. Materials and methods

2.1. Animals and diets

Apc Min/+ mice in the C57BL/6J background were obtained from The Jackson Laboratory (Bar Harbor, ME, USA). *Tnfα* −/− mice were maintained in C57BL/6J background [21]. We confirmed that the cell viability of splenocytes from *Tnfα* −/− mice is reduced after the stimulation with phorbol 12-myristate 13-acetate (PMA; 80 nM) and ionomycin (1 μM) when compared with that from *Tnfα* +/+ mice, thus suggesting the distinguishable responses against inflammatory stimuli between *Tnfα* +/+ and *Tnfα* −/− mice. Compound mutant *Apc* Min/+; *Tnfα* −/− mice were generated by breeding *Apc* Min/+; *Tnfα* +/− males to *Apc* +/+; *Tnfα* +/− females. These mice were maintained on a C57BL/6J genetic background to avoid potential strain differences in phenotype. All mice were bred and maintained in a specific pathogen-free animal facility under standard 12:12 h light:dark cycle and fed on a basal diet, CE-2 (CLEA Japan, Inc., Tokyo, Japan), and water *ad libitum* until the termination of the study.

2.2. Experimental procedures

DSS with a molecular weight of 36,000–50,000 (Wako, Osaka, Japan) was dissolved in distilled water at a concentration of 2% (w/v). Initially, 26 *Apc* Min/+; *Tnfα* +/+ mice (14 males and 12 females) and 25 *Apc* Min/+; *Tnfα* −/− mice (14 males and 11 females) were used for the macroscopic and histological study. The animals of these cohorts were given 2% (w/v) DSS in drinking water for 1 week, starting at 5 weeks of age, according to the protocol described in previous report [20]. The DSS-exposed *Apc* Min/+; *Tnfα* +/+ mice and *Apc* Min/+; *Tnfα* −/− mice were then sacrificed at 10 weeks of age for both the macroscopic inspection and histological analysis (Fig. 1a). Next, 20 male *Tnfα* +/+ mice and 19 male *Tnfα* −/− mice were treated with 2% (w/v) DSS in drinking water for 5 days, starting at 5 weeks of age, and then were sacrificed at day 0 (control, five mice in each group), day 10 (the acute phase of colonic inflammation, seven mice in each group) and day 30 (the chronic phase of colon inflammation, eight mice in *Tnfα* +/+ and seven mice in *Tnfα* −/−) after the exposure of DSS in order to compare the induction of pro-inflammatory factors in the presence or absence of *Tnfα* (Fig. 1b). Trinitrobenzene sulfonic acid (TNBS) was also used for another model of colonic inflammation. TNBS colitis was induced in five male *Tnfα* +/+ and six male *Tnfα* −/− mice according to the method of Wirtz et al. [18] with minor modifications. After the TNBS presensitization, the mice were lightly anesthetized, and an infant feeding catheter (3.5 Fr) was then carefully inserted into the colon such that the tip was 4 cm proximal to the anus. Five percent (w/v) in H_2O TNBS solution dissolved in the same volume of 100% ethanol was then slowly administered into the colon lumen through the catheter. The total injection volume was 100 μl in both groups, thus allowing TNBS to reach the entire colon. After the above administration, the mice were kept upside down while being held by their tails for 60 s and then were returned to their cages. All mice were then sacrificed at day 12 for both macroscopic inspection and histological analysis. At autopsy in each group of mice, their large bowel was flushed with saline, and then was excised. The large bowel from the ileocecal junction to the anal verge was measured, cut open longitudinally along the main axis, and then washed with saline. The total tumor number, tumor localization and the size of each tumor were recorded. The tumor volume was calculated as length × width × width × 0.526 [22]. After macroscopic inspection, it was rolled like a "*Swiss roll*" and then fixed overnight in 10% buffered formalin. Paraffin-embedded sections were made using routine procedures.

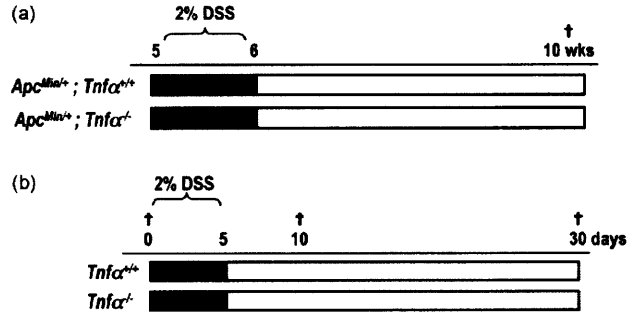

Fig. 1. Experimental protocols for this study. (a) Experimental design to investigate the role of Tnfα in DSS-induced colon tumorigenesis. (■) Basal diet and 2% DSS in drinking water, (□) basal diet and tap water, (†) sacrifice. (b) Experimental design to compare the induction of pro-inflammatory factors in the presence or absence of *Tnfα*. Day 0, day 10 and day 30 represent control, the acute phase of colonic inflammation and the chronic phase of colon inflammation, respectively. (■) Basal diet and 2% DSS in drinking water, (□) basal diet and tap water, (†) sacrifice.

2.3. Histological inflammation score

The histopathological alterations of the colon were examined on hematoxylin and eosin (H&E) stained sections and colon inflamma-

tion was scored according to the following morphological criteria as described previously [23]. Grade 0, normal colon mucosa; Grade 1, shortening and loss of the basal one-third of the actual crypts with mild inflammation and edema in the mucosa; Grade 2, loss of the basal two-thirds of the crypts with moderate inflammation in the mucosa; Grade 3, loss of all crypts with severe inflammation in the mucosa, but with retention of the surface epithelium; and Grade 4, loss of all crypts and surface epithelium with severe inflammation in the mucosa.

2.4. Immunohistochemical analysis

The avidin–biotin peroxidase complex technique was used for immunohistochemical studies. Sections (5 μm thick) were made, deparaffinized, rehydrated in PBS, placed in 10 mmol/l citrate buffer (pH 6.0), and heated in a 750 W microwave four times for 6 min. The endogenous peroxidase activity was blocked by incubation for 10 min in 0.3% H_2O_2. After washing three times with PBS, the sections were then preincubated with 2% bovine serum albumin in PBS for 40 min at room temperature and then incubated with primary antibodies, anti-β-catenin (1:1000; BD Biosciences PharMingen, San Diego, CA, USA), anti-Cox-2 (1:500; Santa Cruz Biotechnology, Santa Cruz, CA, USA) overnight at 4 °C. Subsequently, the sections were incubated with biotinylated secondary antibodies against the primary antibodies (1:250; DAKO Corp., Carpinteria, CA, USA) for 30 min followed by incubation with avidin-coupled peroxidase (Vector Laboratories, Inc., Burlingame, CA, USA) for 30 min at room temperature. The sections were developed with 3,3′-diaminobenzidine (DAB) using DAKO Liquid DAB Substrate-Chromogen System (DAKO) and then were counterstained with hematoxylin, dehydrated, and coverslipped.

2.5. Protein extraction and a Western blot analysis

Total protein was extracted from both the normal colon tissues and the colon tumor tissues, which were excised from *Apc* Min/+; *Tnfα* +/+ and *Apc* Min/+; *Tnfα* −/− mice at autopsy (Fig. 1a), and equivalent amounts of protein (15 μg/lane) were subjected to a Western blot analysis, as described previously [24,25]. The primary antibodies for β-catenin, GAPDH were purchased from BD Biosciences PharMingen (San Diego, CA, USA) and Cell Signaling Technology, Inc. (Danvers, MA, USA), respectively. An antibody against GAPDH served as a loading control.

2.6. Crypt isolation

The excised total colon was washed by PBS several times and cut opened in the longitudinal direction. The total colon was divided into three sections and the distal section was used for crypt isolation. The distal tissue was washed by 1× Hank's Balanced Salt Solution (HBSS; Sigma–Aldrich, St Louis, MO, USA) two times and followed by incubation with 1× HBSS containing 30 mM EDTA at 37 °C for 15 min. After this step, the tissue was dispersed by vortex in the 1× HBSS solution and separated into epithelial crypts and stromal tissues.

2.7. Quantitative real-time reversed transcription-polymerase chain reaction

Total RNA was extracted from the isolated epithelial crypts and stromal tissues of wild-type C57B6/J and Tnfα −/− mice at the indicated time intervals (Fig. 1b) by using the RNAqueous-4PCR kit (Ambion, Austin, TX, USA) according to the manufacturer's protocol. cDNA was synthesized from 1.0 μg of total RNA by using SuperScript III First-Strand Synthesis System (Invitrogen Life Technologies, Carlsbad, CA, USA). Quantitative real-time reverse transcription-polymerase chain reaction (qRT-PCR) amplification was performed in a final volume of 20 μl containing 10 μl of 2× SYBR green master mix (Takara, Kyoto, Japan), 1.0 μl of primers (10 μmol/l), 3.0 μl of distilled water and 5.0 μl of cDNA by using a LightCycler 1.0. (Roche Diagnostics, IN, USA) according to the protocols described previously [26]. The reaction conditions included activation at 95 °C for 10 min, denaturation at 95 °C for 10 s, annealing 60 °C for 10 s and extension 72 °C for 6 s. All PCR amplifications were done for 45 cycles. The expression level of each gene was normalized to the β-actin expression level using the standard curve method. The primer sequences used in qRT-PCR analyses were obtained from the PrimerBank (http://pga.mgh.harvard.edu/primerbank/): for *β-actin*, sense 5′-CATCCGTAAAGACCTCTATGCCAAC-3′ and antisense 5′-ATGGAGCCACCGATCCACA-3′; for *Tnfα*, sense 5′-CCCTCACACTCAGATCATCTTCT-3′ and antisense 5′-GCTACGACGTGGGCTACAG-3′; for *Tnfβ*, sense 5′-CCACCTCTTGAGGGTGCTTG-3′ and antisense 5′-CATGTCGGAGAAAGGCACGAT-3′; for *Ccl2*, sense 5′-TTAAAAACCTGGATCGGAACCAA-3′ and antisense 5′-GCATTAGCTTCAGATTTACGGGT-3′; for *Cxcl1*, sense 5′-CTGGGATTCACCTCAAGAACATC-3′ and antisense 5′-CAGGGTCAAGGCAAGCCTC-3′; for *Cox-2*, sense 5′-TGAGCAACTATTCCAAACCAGC-3′ and antisense 5′-GCACGTAGTCTTCGATCACTATC-3′; for *Il1β*, sense 5′-GCAACTGTTCCTGAACTCAACT-3′ and antisense 5′-ATCTTTTGGGGTCCGTCAACT-3′; and for *Il6*, sense 5′-TAGTCCTTCCTACCCCAATTTCC-3′ and antisense 5′-TTGGTCCTTAGCCACTCCTTC-3′.

2.8. Statistical analysis

The statistical analysis was performed using the GraphPad Prism 4 software program (Graphpad Software, Inc., San Diego, CA, USA). The mean ± SD was calculated for all parameters determined. Statistical significance was evaluated using either Student's *t*-test or Welch's *t*-test for paired samples. p values <0.05 were considered to be statistically significant.

3. Results

3.1. Genetic ablation of Tnfα did not suppress both the colonic inflammation and the expression of pro-inflammatory factors in the colon of mice exposed to DSS

A previous study revealed that *Tnfr1* deficient mice are resistant to the DSS-induced colitis. In the present study, two cohorts of *Apc* Min/+ mice with different *Tnfα* status (*Apc* Min/+; *Tnfα* +/+, *Apc* Min/+; *Tnfα* −/− mice) were exposed to 2% DSS in drinking water for 1 week and sacrificed at the point of week 5 (Fig. 1a). In contrast to the *Tnfr1* deficient mice, mice lacking *Tnfα*, as well as the control mice, exhibited profound body weight loss and bloody diarrhea during the course of DSS treatment. In addition, there were no significant differences in either the physical findings or mortality between *Apc* Min/+; *Tnfα* +/+ and *Apc* Min/+; *Tnfα* −/− mice. There were no apparent differences in either microscopic appearance of the inflamed colon (data not shown) or the histological inflammation score (1.17 ± 0.83 and 1.25 ± 0.97, respectively, p: 0.82) between these two cohorts.

We also examined the effect of *Tnfα* ablation on intestinal inflammation using the trinitrobenzene sulfonic acid (TNBS)-induced model, a different model of intestinal inflammation. However, we could not detect any differences in the histological inflammation score between *Tnfα* +/+ and *Tnfα* −/− mice (2.75 ± 1.50 and 2.50 ± 1.22, respectively, p: 0.78).

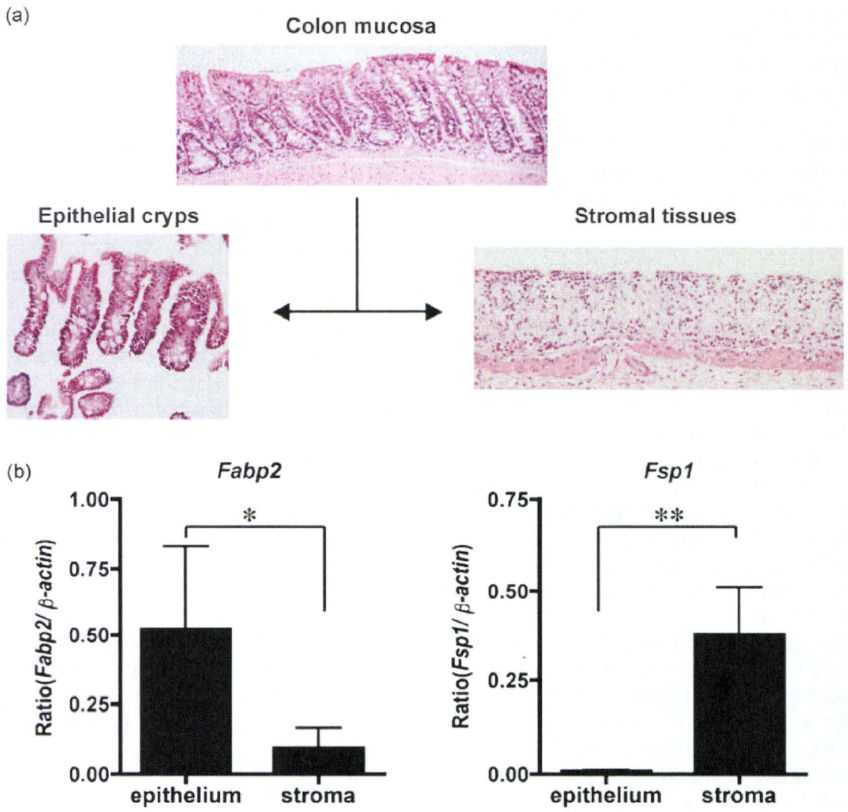

Fig. 2. Crypt isolation and the expression of epithelial or stromal marker gene. (a) Distal colon tissues were separated into epithelial crypts and stromal tissues by crypt isolation as described in Section 2. (b) Quantitative RT-PCR was performed on total RNAs extracted from both epithelial cryps and stromal tissues. The levels of FABP2 and FSP-1 mRNA were normalized to β-actin mRNA levels. Representative results from three independent experiments are shown here. Data represent the mean ± SD. Statistical significance of differences was evaluated by Student's *t*-test with Welch's correction. $^{*}p < 0.05$, $^{**}p < 0.01$.

Both wild-type and *Tnfα* deficient mice were treated with 2% DSS for 5 days and then were sacrificed at day 0 (control), day 10 (the acute phase of colonic inflammation) and day 30 (the chronic phase of colon inflammation; Fig. 1b) in order to compare the induction of pro-inflammatory factors in the presence or absence of *Tnfα*. The crypts were isolated to separate the colons into the epithelial crypts and stromal tissues (Fig. 2a). After crypt isolation, RNA was extracted from these tissue specimens and real-time PCR was used to compare the expression of pro-inflammatory factors between wild-type and *Tnfα* deficient mice. The epithelial marker, *fatty-acid-binding-protein-2* (*Fabp2*) [27–29], was predominantly expressed by RNAs from colonic crypts, whereas the mesenchymal marker, *fibroblast-specific-protein-1* (*Fsp1*), was predominantly expressed at those from stromal tissues (Fig. 2b). These findings indicate that epithelial cells were therefore successfully separated from stromal cells.

The expression of pro-inflammatory factors (*Tnfα*, *Tnfβ*, *Ccl2*, *Cxcl1*, *Il1β*, *Il6*, *Cox-2*) were up-regulated after the DSS exposure in wild-type mice and such altered expression was maintained at a high level until day 30 (Fig. 3a). As expected, during the course of DSS treatment (Fig. 1b), the expression of *Tnfα* was not detectable in either the epithelial or stromal tissues of *Tnfα* deficient mice (Fig. 3b). However, in spite of the lack of *Tnfα* expression, there were no significant differences in the expression of *Tnfβ*, *Ccl2*, *Cxcl1*, *Il1β*, *Il6* and *Cox-2* in either the epithelial or stromal tissues between the wild-type and *Tnfα* deficient mice (Fig. 3c). These results indicate that the genetic ablation of *Tnfα* did not influence either the severity of colitis or the expression of DSS-induced pro-inflammatory factors.

3.2. Genetic ablation of Tnfα did not suppress the infiltration of Cox-2-expressing inflammatory cells and the accumulation of β-catenin protein in the inflamed colorectal tumor tissues

The coordinated activation of the Apc/β-catenin pathway and the Cox-2 signaling pathway plays an important role in colon tumor formation and progression [30]. A previous study revealed a lack of *Tnfr1* to lead to the decreased expression of Cox-2 in the stromal tissues and the decreased expression of nuclear β-catenin in the colonic tumor cells [11]. Therefore, the infiltration of Cox-2-expressing inflammatory cells and the accumulation of nuclear β-catenin was examined by immunostaining. In contrast to previous data, no significant differences were observed in the infiltration index of Cox-2-positive inflammatory cells between *Apc* Min/+; *Tnfα* +/+ and *Apc* Min/+; *Tnfα* −/− mice (42.62 ± 6.65 and 45.73 ± 2.90 cells per field at 400× magnification, respectively, *p*: 0.32) (Fig. 4a). The accumulation of nuclear β-catenin protein in colon tumor cells was not different between the two cohorts (Fig. 4b). In addition, Western blotting revealed the expression of β-catenin protein in colonic tumors to not change between *Apc* Min/+; *Tnfα* +/+ and *Apc* Min/+; *Tnfα* −/− mice (Fig. 4c).

3.3. The genetic ablation of Tnfα did not suppress the inflammation-related colon tumorigenesis

Tnfr1 deficient mice markedly attenuate tumor formation induced by azoxymethane (AOM) and DSS in comparison to wild-type mice [11]. In the present study, as in a previous report [20], colon tumors were detectable only in *Apc* Min/+ mice exposed to

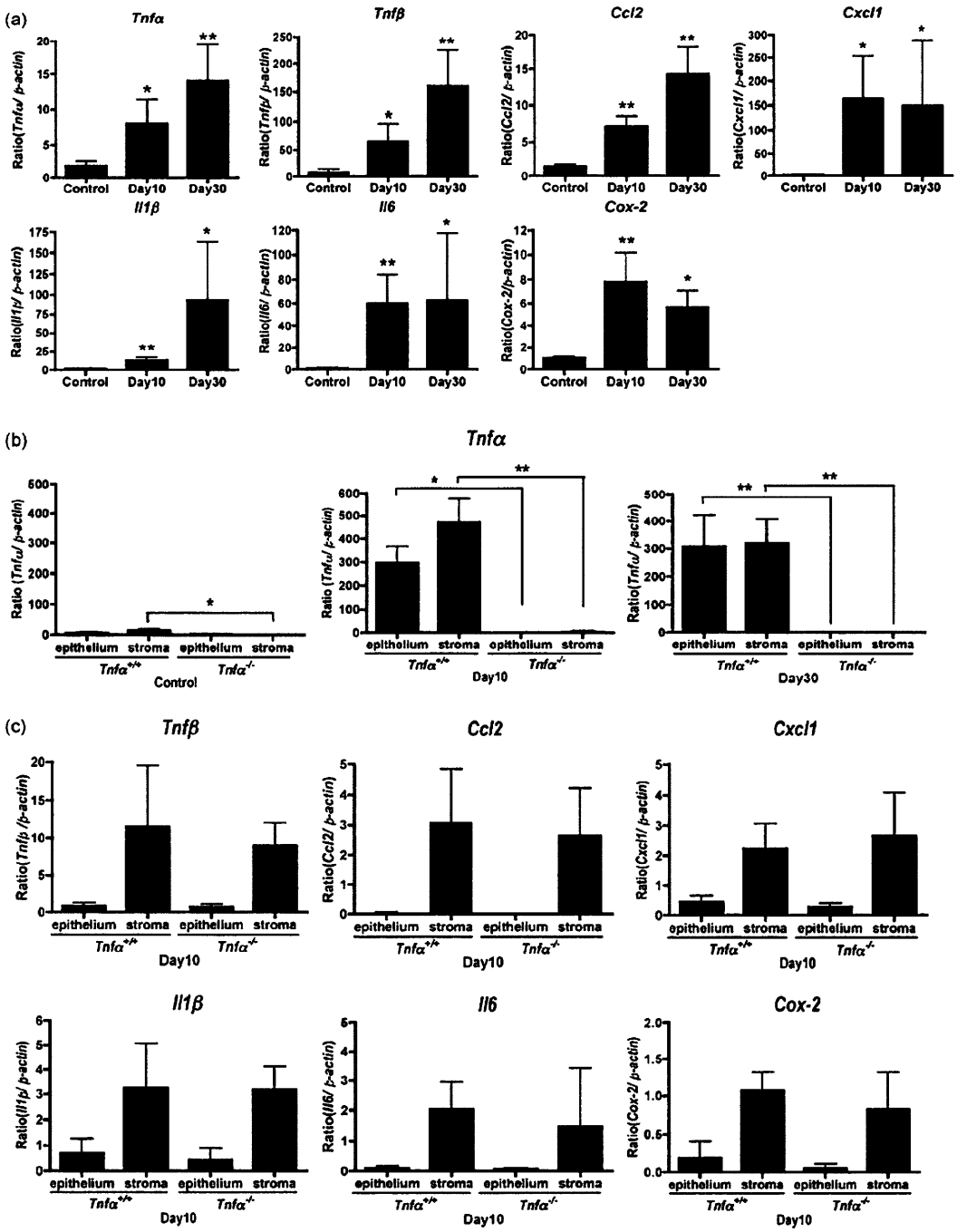

Fig. 3. Pro-inflammatory factor gene expression in the colon. Quantitative RT-PCR was performed on total RNAs extracted from stromal tissues of wild-type mice (a), epithelial and stromal tissues of both wild-type and Tnfα$^{-/-}$ mice (b and c) at the indicated time intervals as indicated. The levels of each pro-inflammatory factor were normalized to β-actin mRNA levels. Representative results from three independent experiments are shown here. Data represent the mean ± SD. Statistical significance of differences was evaluated by Student's *t*-test with Welch's correction (a–c). $^{*}p < 0.05$, $^{**}p < 0.01$.

DSS, whereas no tumors were found in *Apc* +/+ mice with the DSS exposure. The incidence and multiplicity of colonic tumors were 100% and 16.15 ± 5.84/mouse in *Apc* Min/+; *Tnfα* +/+ mice and 100% and 14.27 ± 7.71/mouse in *Apc* Min/+; *Tnfα* −/− mice, respectively. The tumor volumes were 3.90 ± 2.55 mm^3 and 3.81 ± 2.49 mm^3 in *Apc* Min/+; *Tnfα* +/+ and *Apc* Min/+; *Tnfα* −/− mice, respectively (Table 1). Importantly, no significant differences were observed in either the tumor incidence and multiplicity or the tumor volumes between *Apc* Min/+; *Tnfα*+/+ and *Apc* Min/+; *Tnfα*−/− mice. Microscopic examinations also failed to detect any histological differences in colon tumors between *Apc* Min/+; *Tnfα* +/+ and *Apc* Min/+; *Tnfα* −/− mice (data not shown). In addition, the incidence and multiplicity of small intestinal tumors did not alter regardless of the *Tnfα* status (100% and 47.0 ± 2.16/mouse in *Apc* Min/+; *Tnfα* +/+ mice and 100% and 48.8 ± 3.59/mouse in *Apc* Min/+; *Tnfα* −/− mice, respectively).

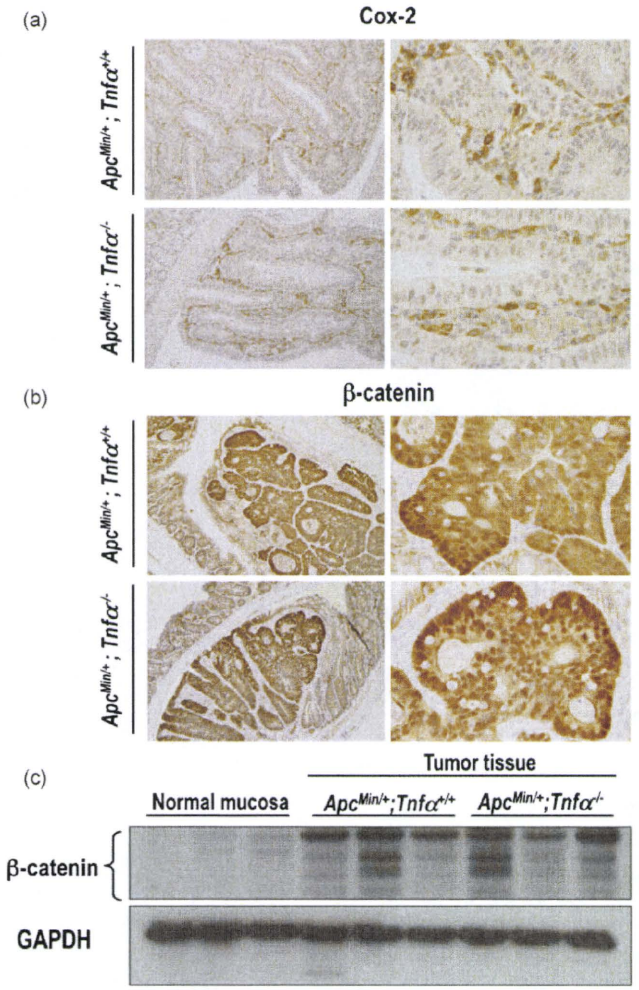

Fig. 4. Cox-2-expressing cells and β-catenin nuclear accumulation in the colon tumor tissues. Colons were immunostained with anti-Cox-2 (a) or anti-β-catenin antibody (b) and representative results from five independent animals are shown here. Original magnification, 100× (left panels), 400× (right panels), respectively. (c) Western blot analysis with anti-β-catenin antibody was performed on cell lysates from both normal colon mucosa and colon tumor tissues. Representative results from three independent experiments are shown here.

4. Discussion

Tnfα is a hormone with a broad spectrum of biological activities, produced mainly by activated macrophages and a variety of other cell types, including activated T cells, mast cells, neutrophils, and astrocytes [31]. Once the protein is efficiently exported from the producing cell, it enters the circulation, where it has a very limited half-life and binds to either high-affinity 55-kDa TNF-receptor-1 (Tnfr1) or low-affinity 75-kDa TNF-receptor-2 (Tnfr2) [32,33]. Popivanova et al. revealed that mice lacking *Tnfr*1 treated with AOM and DSS showed reduced mucosal damage, reduced infiltration of macrophages and neutrophils, and attenuated subsequent tumor formation [11]. These findings indicate Tnfα/Tnfr1 signaling as a crucial mediator of the initiation and promotion of colitis-associated colon carcinogenesis, and suggest that targeting Tnfα may be a useful strategy for prevention and/or treatment of colon cancer in the individuals with IBD.

Table 1
Incidence, multiplicity and tumor volume of large intestinal tumors at week 5.

Genotype	Incidence	Multiplicity[a]	Tumor volume[b]
$Apc^{Min/+}$; $Tnf\alpha^{+/+}$	26/26, 100%	16.15 ± 5.84	3.90 ± 2.25
$Apc^{Min/+}$; $Tnf\alpha^{-/-}$	25/25, 100%	14.27 ± 7.71	3.81 ± 2.49

Statistical significance of differences was evaluated by Student's *t*-test.
[a] Number of tumors/mouse, the mean ± SD.
[b] Tumor volume was calculated as length × width × width × 0.526, the mean ± SD.

In contrast [11], the current study revealed that, despite a deficiency in the *Tnfα* expression, both chemically induced colonic inflammation and the tumor formation in *Tnfα* deficient mice were not attenuated in comparison to those of *Tnfα* +/+ control mice. In addition, the expression of pro-inflammatory factors in the colon mucosa exposed to DSS was not altered in comparison to wild-type control mice. Moreover, no significant differences were observed in either the infiltration of Cox-2-positive inflammatory cells or the nuclear β-catenin accumulation of tumor cells between *Apc* Min/+:*Tnfα* +/+ and *Apc* Min/+:*Tnfα* −/− mice, both of which have been shown to be significantly suppressed in *Tnfr*1 deficient mice [11].

Although Tnfα is the ligand for the Tnfr1, it is noteworthy that Tnfr1 also binds with tumor necrosis factor-β (Tnfβ) or lymphotoxin (LT) [34]. Tnfβ shares about 30% structural homology with Tnfα [35,36], and Tnfα and Tnfβ are functionally indistinguishable with respect to receptor binding and activation of Nf-kB in HL60 cells [37]. Although DSS-induced *Tnfβ* expression was almost equal in both wild-type and *Tnfα* deficient mice, it might be possible that Tnfβ is involved in the induction of colonic inflammation and inflammation-related colon tumorigenesis induced by DSS. This finding is consistent with the previous findings that activation of Nf-kB is associated with DSS-induced inflammation-related colon tumorigenesis [13,38] and that the maximum activation of Nf-kB with Tnfα and/or Tnfβ requires only a small fraction of the total number of Tnf-receptors to be occupied [39].

Previous studies demonstrated that several inflammation-related factors including *Il*1β, Stat3 and iNOS are involved in DSS-induced inflammation-related colon tumorigenesis [38,40,41]. In addition, the possible interaction between iNOS, TnFα and *Il*1β is suggested to play a role in the tumor promotion of inflammation-related colon carcinogenesis [42]. Given such intricate inflammatory responses, it is also possible that the Tnfα-independent signal may promote the inflammation-related mouse colon tumorigenesis in the present study.

There is increasing evidence that the anti-Tnfα monoclonal antibody, infliximab, is an effective therapy for IBD, including Crohn's disease and ulcerative colitis [43–49]. Infliximab is a chimeric monoclonal antibody that binds not only the soluble subunit of Tnfα but also the membrane-bound precursor of Tnfα [50,51]. Infliximab inhibits a broad range of biological activities of Tnfα by blocking the interaction of Tnfα with its receptors. Given the fact that the genetic deletion for *Tnfr*1 significantly suppressed inflammation-related colon tumorigenesis, it was expected that the blockage for Tnfα with the use of infliximab could be a useful strategy for both the chemoprevention and therapy for tumorigenesis. Indeed, previous studies demonstrated that antibodies against Tnfα strongly suppress the development of inflammation-related CRC [11,15]. In contrast, the current study revealed that the genetic ablation of Tnfα alone did not either reduce colon inflammation or attenuate tumor formation. Our results may therefore suggest that an indirect action of anti-Tnfα antibodies exerts a tumor suppressive effect in inflammation-related CRC. A previous study demonstrated that anti-Tnfα monoclonal antibody binds to the transmembrane form of Tnfα, thus resulting in the efficient killing of the Tnfα-expressing cells by both antibody-dependent cellular toxicity and complement-dependent cytotoxicity effector mechanisms [51,52]. The mode of action of anti-Tnfα monoclonal antibody for the treatment of IBD and IBD-related tumorigenesis might be attributed principally to the lysis of the inflammatory

cells rather than blocking the interaction of Tnfα with its receptors.

In conclusion, the current study revealed that the genetic ablation of *Tnfα* results in no detectable effect on either the suppression of DSS-induced colonic inflammation or the attenuation of inflammation-related mouse colon tumorigenesis. These observations suggest that intricate inflammatory responses are involved in the inflammation-related mouse colon tumorigenesis.

Conflicts of interest

No conflicts of interest.

Acknowledgments

We would like to thank Masanao Saio and Yusuke Kitou for helpful discussions. We would also thank Kyoko Takahashi, Ayako Suga, and Yoshitaka Kinjyo for their valuable technical assistance and animal care. This study was supported by grants from Japan Science and Technology (JST), grants from PRESTO, grants from the Ministry of Health, Labour and Welfare of Japan, and grants from the Ministry of Education, Culture, Sports, Science and Technology of Japan.

References

[1] S.P. Hussain, L.J. Hofseth, C.C. Harris, Radical causes of cancer, Nat. Rev. Cancer 3 (4) (2003) 276–285.
[2] B.A. Lashner, K.S. Provencher, J.M. Bozdech, A. Brzezinski, Worsening risk for the development of dysplasia or cancer in patients with chronic ulcerative colitis, Am. J. Gastroenterol. 90 (3) (1995) 377–380.
[3] R.M. Locksley, N. Killeen, M.J. Lenardo, The TNF and TNF receptor superfamilies: integrating mammalian biology, Cell 104 (4) (2001) 487–501.
[4] E.A. Carswell, L.J. Old, R.L. Kassel, S. Green, N. Fiore, B. Williamson, An endotoxin-induced serum factor that causes necrosis of tumors, Proc. Natl. Acad. Sci. U.S.A. 72 (9) (1975) 3666–3670.
[5] N. Senzer, S. Mani, A. Rosemurgy, J. Nemunaitis, C. Cunningham, C. Guha, N. Bayol, M. Gillen, K. Chu, C. Rasmussen, H. Rasmussen, D. Kufe, R. Weichselbaum, N. Hanna, TNFerade biologic, an adenovector with a radiation-inducible promoter, carrying the human tumor necrosis factor alpha gene: a phase I study in patients with solid tumors, J. Clin. Oncol. 22 (4) (2004) 592–601.
[6] R.J. Moore, D.M. Owens, G. Stamp, C. Arnott, F. Burke, N. East, H. Holdsworth, L. Turner, B. Rollins, M. Pasparakis, G. Kollias, F. Balkwill, Mice deficient in tumor necrosis factor-alpha are resistant to skin carcinogenesis, Nat. Med. 5 (7) (1999) 828–831.
[7] M. Suganuma, S. Okabe, M.W. Marino, A. Sakai, E. Sueoka, H. Fujiki, Essential role of tumor necrosis factor alpha (TNF-alpha) in tumor promotion as revealed by TNF-alpha-deficient mice, Cancer Res. 59 (18) (1999) 4516–4518.
[8] K.A. Scott, R.J. Moore, C.H. Arnott, N. East, R.G. Thompson, B.J. Scallon, D.J. Shealy, F.R. Balkwill, An anti-tumor necrosis factor-alpha antibody inhibits the development of experimental skin tumors, Mol. Cancer Ther. 2 (5) (2003) 445–451.
[9] B. Knight, G.C. Yeoh, K.L. Husk, T. Ly, L.J. Abraham, C. Yu, J.A. Rhim, N. Fausto, Impaired preneoplastic changes and liver tumor formation in tumor necrosis factor receptor type 1 knockout mice, J. Exp. Med. 192 (12) (2000) 1809–1818.
[10] M.S. Naylor, G.W. Stamp, F.R. Balkwill, Investigation of cytokine gene expression in human colorectal cancer, Cancer Res. 50 (14) (1990) 4436–4440.
[11] B.K. Popivanova, K. Kitamura, Y. Wu, T. Kondo, T. Kagaya, S. Kaneko, M. Oshima, C. Fujii, N. Mukaida, Blocking TNF-alpha in mice reduces colorectal carcinogenesis associated with chronic colitis, J. Clin. Invest. 118 (2) (2008) 560–570.
[12] H. Sano, Y. Kawahito, R.L. Wilder, A. Hashiramoto, S. Mukai, K. Asai, S. Kimura, H. Kato, M. Kondo, T. Hla, Expression of cyclooxygenase-1 and -2 in human colorectal cancer, Cancer Res. 55 (17) (1995) 3785–3789.
[13] F.R. Greten, L. Eckmann, T.F. Greten, J.M. Park, Z.W. Li, L.J. Egan, M.F. Kagnoff, M. Karin, IKKbeta links inflammation and tumorigenesis in a mouse model of colitis-associated cancer, Cell 118 (3) (2004) 285–296.
[14] Q. Li, S. Withoff, I.M. Verma, Inflammation-associated cancer: NF-kappaB is the lynchpin, Trends Immunol. 26 (6) (2005) 318–325.
[15] M. Onizawa, T. Nagaishi, T. Kanai, K. Nagano, S. Oshima, Y. Nemoto, A. Yoshioka, T. Totsuka, R. Okamoto, T. Nakamura, N. Sakamoto, K. Tsuchiya, K. Aoki, K. Ohya, H. Yagita, M. Watanabe, Signaling pathway via TNF-alpha/NF-kappaB in intestinal epithelial cells may be directly involved in colitis-associated carcinogenesis, Am. J. Physiol. Gastrointest. Liver Physiol. 296 (4) (2009) G850–859.
[16] S.H. Itzkowitz, X. Yio, Inflammation and cancer IV. Colorectal cancer in inflammatory bowel disease: the role of inflammation, Am. J. Physiol. Gastrointest. Liver Physiol. 287 (1) (2004) G7–17.
[17] M. Kawada, A. Arihiro, E. Mizoguchi, Insights from advances in research of chemically induced experimental models of human inflammatory bowel disease, World J. Gastroenterol. 13 (42) (2007) 5581–5593.
[18] S. Wirtz, C. Neufert, B. Weigmann, M.F. Neurath, Chemically induced mouse models of intestinal inflammation, Nat. Protoc. 2 (3) (2007) 541–546.
[19] L.A. Dieleman, B.U. Ridwan, G.S. Tennyson, K.W. Beagley, R.P. Bucy, C.O. Elson, Dextran sulfate sodium-induced colitis occurs in severe combined immunodeficient mice, Gastroenterology 107 (6) (1994) 1643–1652.
[20] T. Tanaka, H. Kohno, R. Suzuki, K. Hata, S. Sugie, N. Niho, K. Sakano, M. Takahashi, K. Wakabayashi, Dextran sodium sulfate strongly promotes colorectal carcinogenesis in Apc(Min/+) mice: inflammatory stimuli by dextran sodium sulfate results in development of multiple colonic neoplasms, Int. J. Cancer 118 (1) (2006) 25–34.
[21] T. Taniguchi, M. Takata, A. Ikeda, E. Momotani, K. Sekikawa, Failure of germinal center formation and impairment of response to endotoxin in tumor necrosis factor alpha-deficient mice, Lab. Invest. 77 (6) (1997) 647–658.
[22] N.R. Murray, J. Weems, U. Braun, M. Leitges, A.P. Fields, Protein kinase C betaII and PKCiota/lambda: collaborating partners in colon cancer promotion and progression, Cancer Res. 69 (2) (2009) 656–662.
[23] H.S. Cooper, S.N. Murthy, R.S. Shah, D.J. Sedergran, Clinicopathologic study of dextran sulfate sodium experimental murine colitis, Lab. Invest. 69 (2) (1993) 238–249.
[24] M. Shimizu, A. Deguchi, Y. Hara, H. Moriwaki, I.B. Weinstein, EGCG inhibits activation of the insulin-like growth factor-1 receptor in human colon cancer cells, Biochem. Biophys. Res. Commun. 334 (3) (2005) 947–953.
[25] M. Shimizu, A. Deguchi, A.K. Joe, J.F. McKoy, H. Moriwaki, I.B. Weinstein, EGCG inhibits activation of HER3 and expression of cyclooxygenase-2 in human colon cancer cells, J. Exp. Ther. Oncol. 5 (1) (2005) 69–78.
[26] T. Oyama, Y. Yamada, K. Hata, H. Tomita, A. Hirata, H. Sheng, A. Hara, H. Aoki, T. Kunisada, S. Yamashita, H. Mori, Further upregulation of beta-catenin/Tcf transcription is involved in the development of macroscopic tumors in the colon of ApcMin/+ mice, Carcinogenesis 29 (3) (2008) 666–672.
[27] H.M. Shields, M.L. Bates, N.M. Bass, C.J. Best, D.H. Alpers, R.K. Ockner, Light microscopic immunocytochemical localization of hepatic and intestinal types of fatty acid-binding proteins in rat small intestine, J. Lipid Res. 27 (5) (1986) 549–557.
[28] D.A. Sweetser, S.M. Hauft, P.C. Hoppe, E.H. Birkenmeier, J.I. Gordon, Transgenic mice containing intestinal fatty acid-binding protein–human growth hormone fusion genes exhibit correct regional and cell-specific expression of the reporter gene in their small intestine, Proc. Natl. Acad. Sci. U.S.A. 85 (24) (1988) 9611–9615.
[29] A. Haegebarth, W. Bie, R. Yang, S.E. Crawford, V. Vasioukhin, E. Fuchs, A.L. Tyner, Protein tyrosine kinase 6 negatively regulates growth and promotes enterocyte differentiation in the small intestine, Mol. Cell. Biol. 26 (13) (2006) 4949–4957.
[30] M. Oshima, J.E. Dinchuk, S.L. Kargman, H. Oshima, B. Hancock, E. Kwong, J.M. Trzaskos, J.F. Evans, M.M. Taketo, Suppression of intestinal polyposis in Apc delta716 knockout mice by inhibition of cyclooxygenase 2 (COX-2), Cell 87 (5) (1996) 803–809.
[31] P.W. Szlosarek, F.R. Balkwill, Tumour necrosis factor alpha: a potential target for the therapy of solid tumours, Lancet Oncol. 4 (9) (2003) 565–573.
[32] B.A. Beutler, I.W. Milsark, A. Cerami, Cachectin/tumor necrosis factor: production, distribution, and metabolic fate in vivo, J. Immunol. 135 (6) (1985) 3972–3977.
[33] S. de Kossodo, G.E. Grau, J.A. Louis, I. Muller, Tumor necrosis factor alpha (TNF-alpha) and TNF-beta and their receptors in experimental cutaneous leishmaniasis, Infect. Immun. 62 (4) (1994) 1414–1420.
[34] L.A. Tartaglia, D.V. Goeddel, Two TNF receptors, Immunol. Today 13 (5) (1992) 151–153.
[35] M.J. Eck, M. Ultsch, E. Rinderknecht, A.M. de Vos, S.R. Sprang, The structure of human lymphotoxin (tumor necrosis factor-beta) at 1.9-A resolution, J. Biol. Chem. 267 (4) (1992) 2119–2122.
[36] J. Browning, A. Ribolini, Studies on the differing effects of tumor necrosis factor and lymphotoxin on the growth of several human tumor lines, J. Immunol. 143 (6) (1989) 1859–1867.
[37] H.P. Hohmann, R. Kolbeck, R. Remy, A.P. van Loon, Cyclic AMP-independent activation of transcription factor NF-kappa B in HL60 cells by tumor necrosis factors alpha and beta, Mol. Cell. Biol. 11 (4) (1991) 2315–2318.
[38] M. Kim, S. Miyamoto, Y. Yasui, T. Oyama, A. Murakami, T. Tanaka, Zerumbone, a tropical ginger sesquiterpene, inhibits colon and lung carcinogenesis in mice, Int. J. Cancer 124 (2) (2009) 264–271.
[39] M.M. Chaturvedi, M. Higuchi, B.B. Aggarwal, Effect of tumor necrosis factors, interferons, interleukins, and growth factors on the activation of NF-kappa B: evidence for lack of correlation with cell proliferation, Lymphokine Cytokine Res. 13 (5) (1994) 309–313.
[40] T. Tanaka, R. Suzuki, H. Kohno, S. Sugie, M. Takahashi, K. Wakabayashi, Colonic adenocarcinomas rapidly induced by the combined treatment with 2-amino-1-methyl-6-phenylimidazo[4,5-b]pyridine and dextran sodium sulfate in male ICR mice possess beta-catenin gene mutations and increases immunoreactivity for beta-catenin, cyclooxygenase-2 and inducible nitric oxide synthase, Carcinogenesis 26 (1) (2005) 229–238.
[41] T. Tanaka, Y. Yasui, M. Tanaka, T. Oyama, K.M. Rahman, Melatonin suppresses AOM/DSS-induced large bowel oncogenesis in rats, Chem. Biol. Interact. 177 (2) (2009) 128–136.
[42] H. Kohno, M. Takahashi, Y. Yasui, R. Suzuki, S. Miyamoto, Y. Kamanaka, M. Naka, T. Maruyama, K. Wakabayashi, T. Tanaka, A specific inducible nitric oxide synthase inhibitor, ONO-1714 attenuates inflammation-related large bowel carcinogenesis in male Apc(Min/+) mice, Int. J. Cancer 121 (3) (2007) 506–513.
[43] D.H. Present, P. Rutgeerts, S. Targan, S.B. Hanauer, L. Mayer, R.A. van Hogezand, D.K. Podolsky, B.E. Sands, T. Braakman, K.L. DeWoody, T.F. Schaible, S.J. van

Deventer, Infliximab for the treatment of fistulas in patients with Crohn's disease, N. Engl. J. Med. 340 (18) (1999) 1398–1405.
[44] S.B. Hanauer, B.G. Feagan, G.R. Lichtenstein, L.F. Mayer, S. Schreiber, J.F. Colombel, D. Rachmilewitz, D.C. Wolf, A. Olson, W. Bao, P. Rutgeerts, Maintenance infliximab for Crohn's disease: the ACCENT I randomised trial, Lancet 359 (9317) (2002) 1541–1549.
[45] C. Su, B.A. Salzberg, J.D. Lewis, J.J. Deren, A. Kornbluth, D.A. Katzka, R.B. Stein, D.R. Adler, G.R. Lichtenstein, Efficacy of anti-tumor necrosis factor therapy in patients with ulcerative colitis, Am. J. Gastroenterol. 97 (10) (2002) 2577–2584.
[46] L. de Ridder, J.C. Escher, J. Bouquet, J.J. Schweizer, E.H. Rings, J.J. Tolboom, R.H. Houwen, O.F. Norbruis, B.H. Derkx, J.A. Taminiau, Infliximab therapy in 30 patients with refractory pediatric crohn disease with and without fistulas in The Netherlands, J. Pediatr. Gastroenterol. Nutr. 39 (1) (2004) 46–52.
[47] P. Rutgeerts, G. Van Assche, S. Vermeire, Optimizing anti-TNF treatment in inflammatory bowel disease, Gastroenterology 126 (6) (2004) 1593–1610.
[48] T.N. Brooklyn, M.G. Dunnill, A. Shetty, J.J. Bowden, J.D. Williams, C.E. Griffiths, A. Forbes, R. Greenwood, C.S. Probert, Infliximab for the treatment of pyoderma gangrenosum: a randomised, double blind, placebo controlled trial, Gut 55 (4) (2006) 505–509.
[49] A Swaminath, S. Lichtiger, Dilation of colonic strictures by intralesional injection of infliximab in patients with Crohn's colitis, Inflamm. Bowel Dis. 14 (2) (2008) 213–216.
[50] D.M. Knight, H. Trinh, J. Le, S. Siegel, D. Shealy, M. McDonough, B. Scallon, M.A. Moore, J. Vilcek, P. Daddona, et al., Construction and initial characterization of a mouse–human chimeric anti-TNF antibody, Mol. Immunol. 30 (16) (1993) 1443–1453.
[51] B.J. Scallon, M.A. Moore, H. Trinh, D.M. Knight, J. Ghrayeb, Chimeric anti-TNF-alpha monoclonal antibody cA2 binds recombinant transmembrane TNF-alpha and activates immune effector functions, Cytokine 7 (3) (1995) 251–259.
[52] S.A. Siegel, D.J. Shealy, M.T. Nakada, J. Le, D.S. Woulfe, L. Probert, G. Kollias, J. Ghrayeb, J. Vilcek, P.E. Daddona, The mouse/human chimeric monoclonal antibody cA2 neutralizes TNF in vitro and protects transgenic mice from cachexia and TNF lethality in vivo, Cytokine 7 (1) (1995) 15–25.